SOLAR NEUTRINOS – footnote

- hep neutrinos

$$^3He + p \rightarrow {}^4He + e^+ + \nu_e$$

$(E_\nu < 18.8\,MeV)$

weak alternative to pp I termination via

$$^3He + {}^3He \rightarrow {}^4He + 2p$$

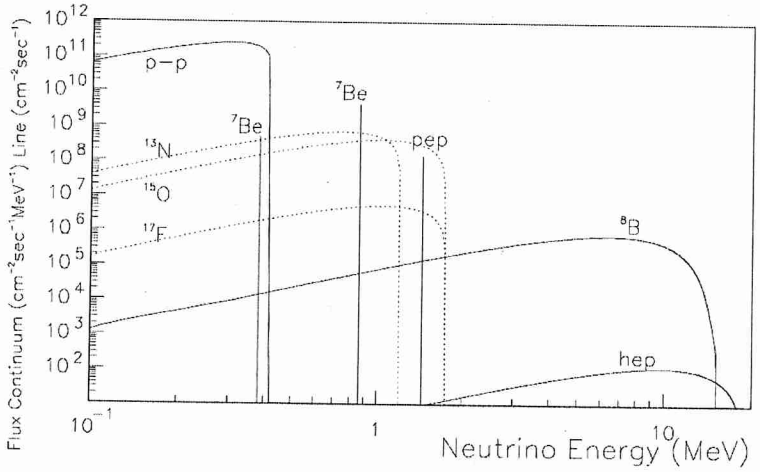

Figure 1: The solar neutrino spectrum calculated by the BP98 standard solar model [4]. Several tens of billions of solar neutrinos traverse a square cm of the earth each second.

EXPLOSNE NUCLEOSYNTHESIS

1970s

- PARAMETERIZED CALCULATIONS for He, C, ... Si LAYERS
- CHOOSE INITIAL MIX WITH ONE GOAL BEING TO MATCH SOLAR COMPOSITION

1985+

- ENS INCORPORATED INTO SN II & SN Ia MODELS following hydrostatic burning
- EXPLORE RANGE OF MODELS
  - ONE AIM: REPRODUCE SOLAR COMPOSITION

now

- **HYDRODYNAMIK SIMULATIONS**

ENS	1970s

for SN II

INITIAL CONDITIONS: T, ρ, comp (incl. γ)

picked from 'models' of pre-SN

TIMESCALE: mark of free-fall τ_{ff}

HOMOLOGOUS EXPANSION

$\Delta r \propto r \rightarrow \frac{r}{r_0} = \left(\frac{\rho_0}{\rho}\right)^{1/3}$

DEFINE $\tau_{HD} = \tau_{ff} = \frac{1}{d \ln \rho / dt}$

$= -\frac{1}{3}\left(\frac{r}{\dot{r}}\right)$

EQN OF MOTION

$$\ddot{r} = \frac{1}{2}\frac{d\dot{r}^2}{dt} = -\frac{GM(r_0)}{r^2}$$

$$\dot{r} = \sqrt{2GM(r_0)}\left(\frac{1}{r} - \frac{1}{r_0}\right)^{1/2}$$

$$\tau_{HO}^{-1} = 3\frac{\dot{r}}{r} \quad ; M(r_0) = \frac{4}{3}\pi r_0^3 \rho_0$$

$$\frac{r}{r_0} = (\rho_0/\rho)^{1/3}$$

$$\tau_{HO}^{-1} = \sqrt{24G\pi\rho_0}\left[\frac{\rho}{\rho_0}\left(1 - \frac{\rho_0}{\rho}\right)^{1/3}\right]^{1/2}$$

slowly var.

$$\tau_{HO} \approx \frac{1}{\sqrt{24\pi G\rho_0}} = \frac{446}{\sqrt{\rho_0}} \quad [5]$$

for ρ in g/cm^3

NUCLEAR PHYSICS ISSUES

- MANY uncertainties, esp. away from valley of stability — PROTON DRIPLINE
- EXPERIMENTS ADVANCING RAPIDLY

  RADIOACTIVE NUCLEI BEAMS

WHERE ?

CLASSICAL NOVAE for HOT CNO

- Thermonuclear runaway in partially e- degenerate gas

  $T \sim (1-2)\,10^8$ K [C-O WD]

  $\sim (4-5)\,10^8$ K [ONeMg WD]

  $t \sim 100-200$ s

- Source of trace nuclides

  ^7Li, ^{15}N, ^{18}O, $^{22}Ne^*$, $^{26}Al^*$

  $\Delta M_{ej} \sim 2 \times 10^{-5} M_\odot$ but

  1 nova per 30yr in the Galaxy

X-ray BURSTERS

- Hot CNO-cycles with breakout to higher Z via αp- and rp-processes with fueling by the 3α-process

- THERMONUCLEAR EXPLOSION ON ACCRETING NEUTRON STAR

$T \sim (7-15)\ 10^8$ K (+STABLE BURNING)

$\rho \sim 10^6 - 10^8$ g/cm^3

$t \sim 5 - 10$ s

- 'NO' N'SYNTHESIS CONSEQUENCES ON GALACTIC SCALE
  - DEEP POTENTIAL WELL
    ∴ EJECTA CANNOT ESCAPE NEUTRON STAR ?
  - BUT V. HIGH YIELDS FOR p-RICH NUCLIDES

SN II from MASSIVE STARS

- LAYERS subjected to EXPLOSIVE N' SYNTHESIS

SN Ia

CLASSICAL NOVAE

- THERMONUCLEAR RUNAWAYS on the surface of a white dwarf in a binary.
- WD accretes gas from its companion which fills its Roche lobe
- ACCRETED material forms thin dense layer which is e-degenerate
- DREDGE-UP into the layer from below
  ^4He, ^{12}C, ^{16}O for CO WD
  ^{16}O, ^{20}Ne, ^{24}Mg for ONeMg
  (required not predicted?)
- CRITICAL MASS → THERMONUCLEAR IGNITION $(m_{WD}, \dot{m})$
  - PP CHAIN
  - CNO cycles until e.deg. lifted
- T↑ rapidly → convective zone at bottom of the hot layer → β^+ products to surface

- Typically,

  $\rho \sim 10^3$ g/cm^3

  $T_{pk} \sim (1-4)\, 10^8$ K

- THEN, ($T_{pk} \lesssim 4 \times 10^8$ K)
  no breakouts from CNO or hot CNO because $(p,\alpha) > (p,\gamma)$ at ^{18}F and ^{19}F and α-capture unlikely when H fuel is left.

  - MATERIAL EJECTED
    then ACCRETION resumes and NOVAE may repeat

HOT CNO CYCLES

- CYCLE TIME OF HOT-1 set by β^+ DECAYS OF ^{14}O AND ^{15}O → WAITING POINTS
  $\simeq$ 278 secs
- ENERGY GENERATION set by total time for a cycle (β^+ decays)
- No breakout for $T \lesssim 400 \times 10^6$ K

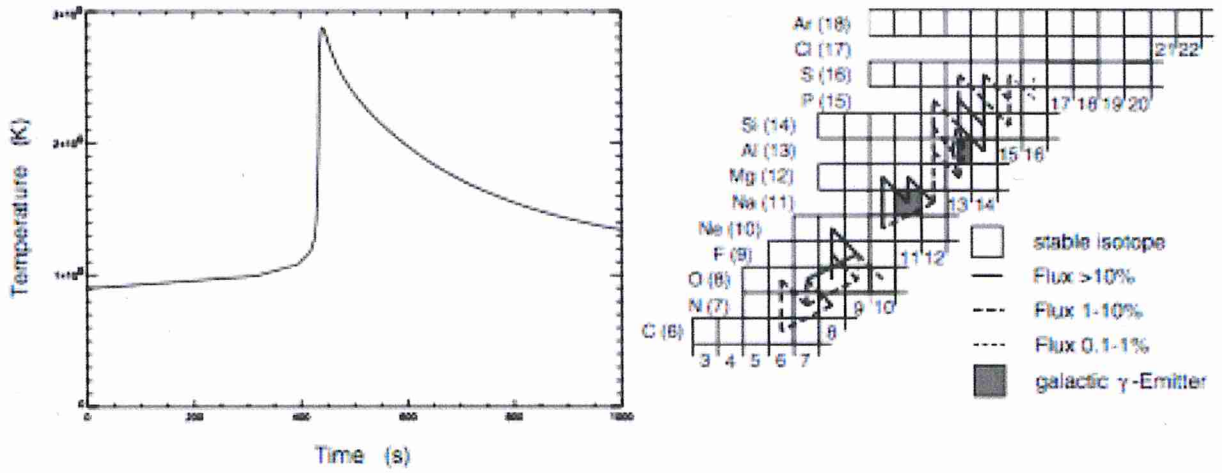

Figure 11. The left-hand panel shows the temperature curve during the thermonuclear runaway of a nova. The right-hand panel indicates the nuclear burning path associated with the thermonuclear runaway. While the main bulk of the energy generation is provided by the hot CNO cycles, interesting nucleosynthesis aspects are expected from the NeNa and the MgAl cycles, which are triggered by proton capture processes on Ne and Mg material mixed in from an O–Ne–M white dwarf.

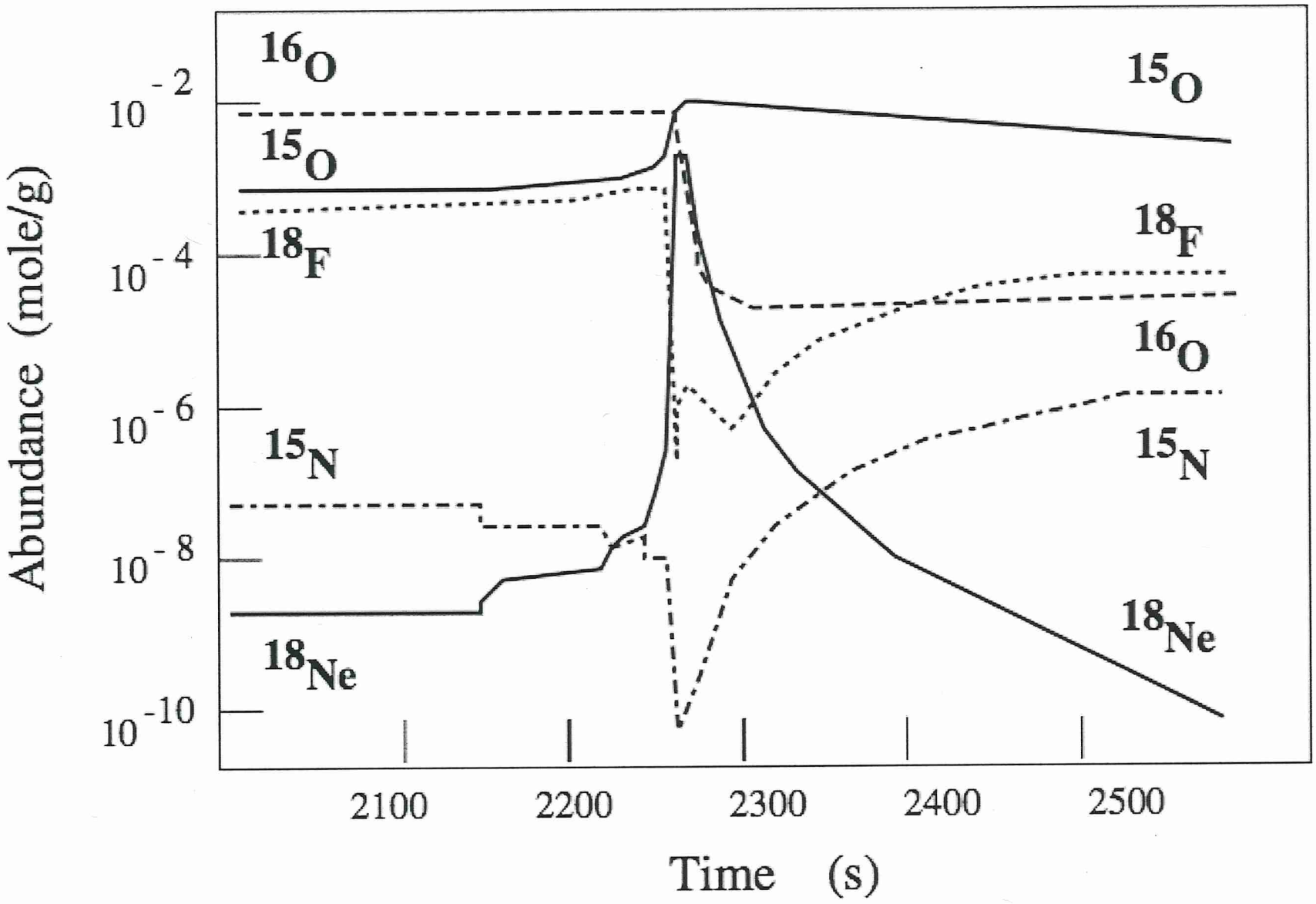

Figure 12. Nucleosynthesis of CNO isotopes during a nova explosion.

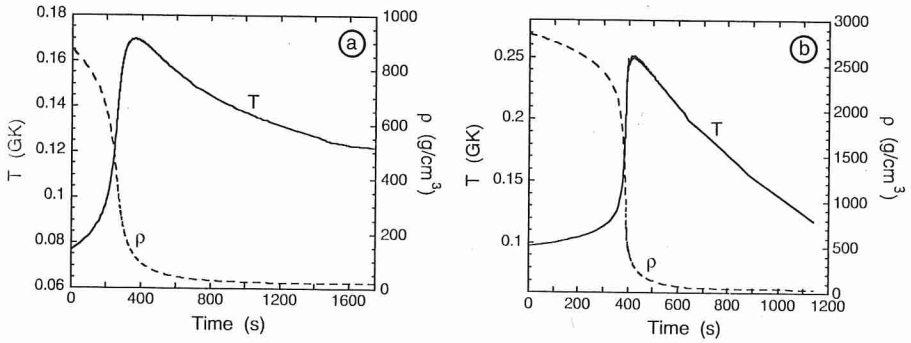

Fig. 5.25 Temperature and density evolution of the hottest hydrogen-burning zone during the thermonuclear runaway on the surface of a white dwarf with (a) $M = 1.0\ M_{(\cdot)}$ and CO composition, and (b) $M = 1.25\ M_{(\cdot)}$ and ONe composition. The curves are adopted from hydrodynamic simulations of classical nova explosions (José and Hernanz 1998).

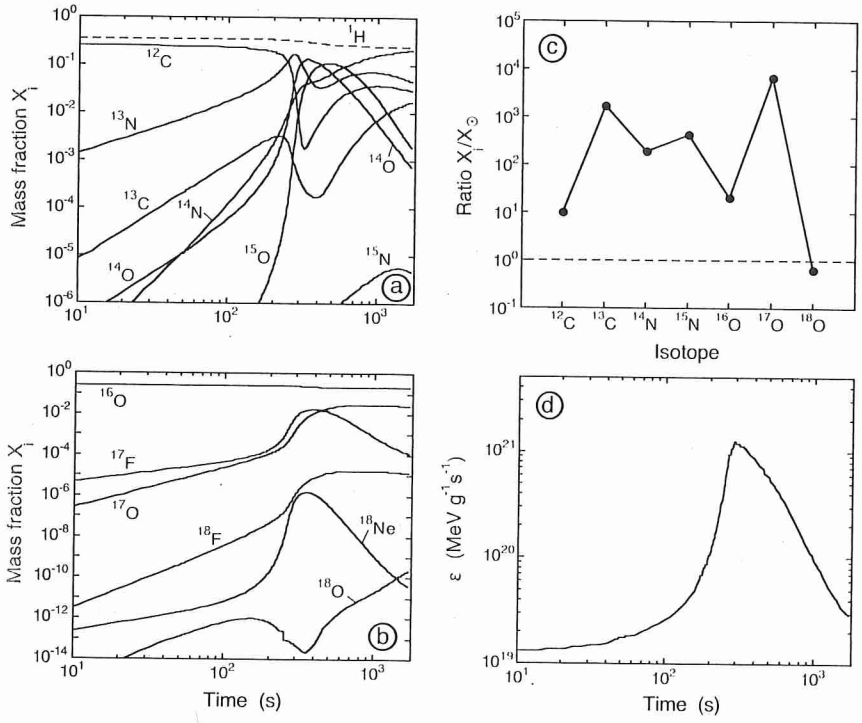

Fig. 5.26 Explosive hydrogen burning during the thermonuclear runaway on the surface of a CO white dwarf. The results show the operation of the HCNO cycles and are obtained by performing a numerical reaction network calculation using the temperature and density evolution for the hottest zone displayed in Fig. 5.25a. (a), (b) Abundance evolutions in the $A \lesssim 20$ mass region; (c) ratios of final mass fractions, after all β^+-decays have been completed, and the corresponding solar system mass fractions; (d) time evolution of the energy generation rate.

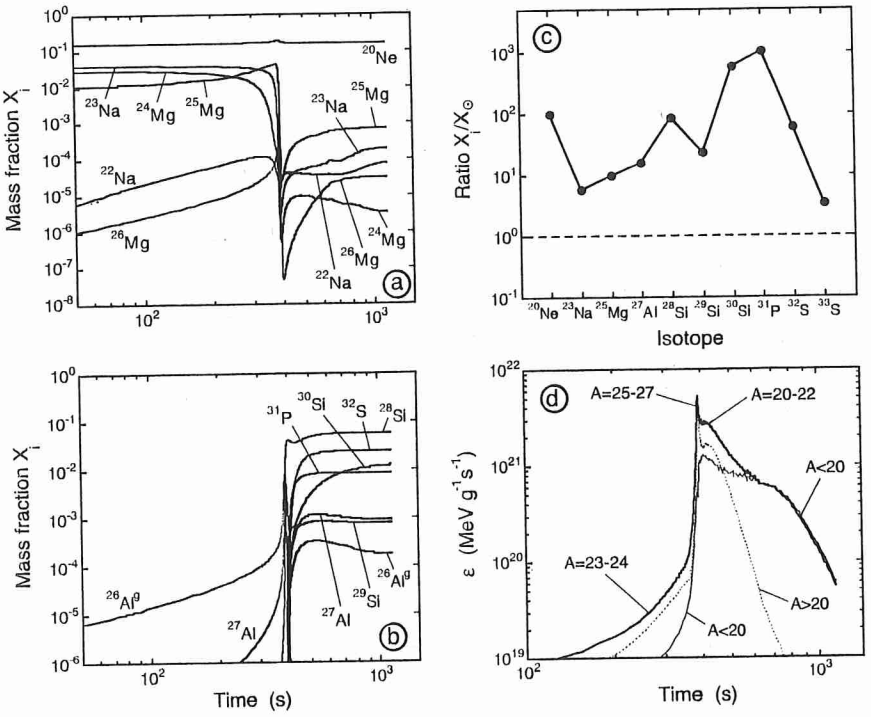

Fig. 5.28 Explosive hydrogen burning during the thermonuclear runaway on the surface of a ONe white dwarf. The results show the operation of nuclear processes in the $A \geq 20$ region and are obtained from a numerical reaction network calculation using the temperature and density evolution for the hottest zone displayed in Fig. 5.25b. (a), (b) abundance evolutions in the $A \geq 20$ mass region; (c) ratios of final mass fractions, after all β^+-decays have been completed, and the corresponding solar system mass fractions; (d) time evolution of the energy generation rate.

DO PREDICTED ABUNDANCES = OBSERVED ?

- NOT EASY TO GET ACC. ABUNDANCES
  BUT Ne–S up (ONeMg WD)
  N (OC WD)

- REQUIRE AD HOC MIXING WITH WD SURFACE

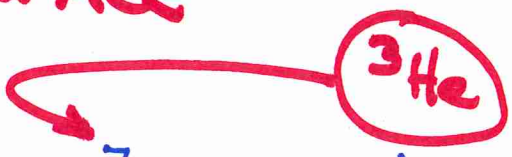

* RECENT ^7Be and ^7Li DETECTIONS
  → GIVES Li vs Fe relation?

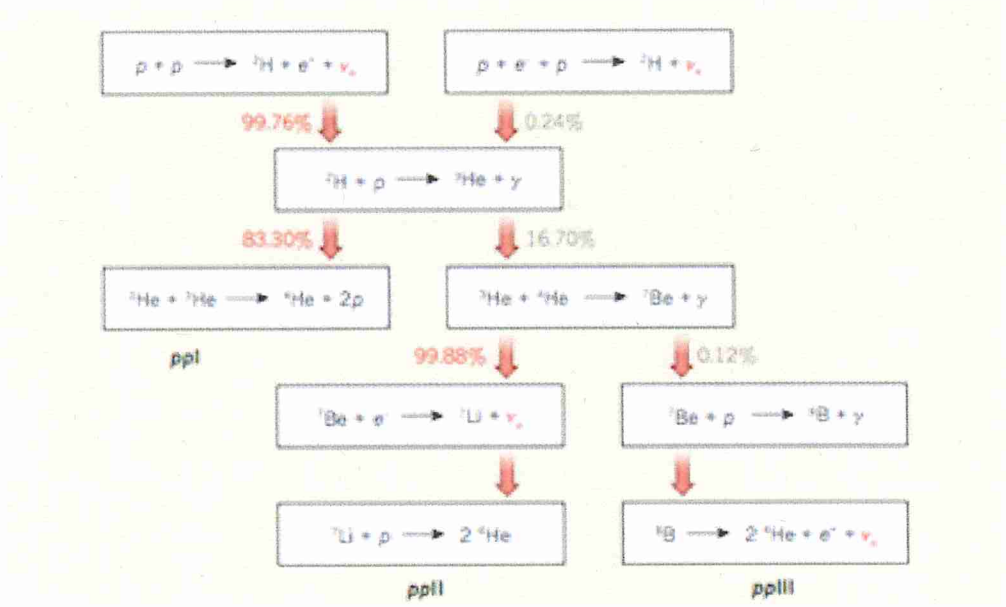

Figure 1 | The *pp* chain. The proton–proton (*pp*) chain of reactions is the dominant mechanism by which four protons are fused in the Sun to produce ^{4}He. Its three cycles, labelled *ppI*, *ppII* and *ppIII*, are each accompanied by a distinctive electron neutrino (ν_e). In cases in which two reactions compete, the relative percentages of the two branches are indicated (taken from the standard solar model[12]). *p*, Proton; ^{2}H, deuterium; e^+, positron; e^-, electron; γ, γ-ray; ^{3,4}He, helium-3 and -4; ^{7}Be, beryllium-7; ^{7}Li, lithium-7; ^{8}B, boron-8. The Borexino Collaboration[7] reports the first measurement of the neutrinos associated with the *p*+*p* reaction, and earlier measured the neutrinos from the ^{7}Be and $p + e^- + p$ reactions.

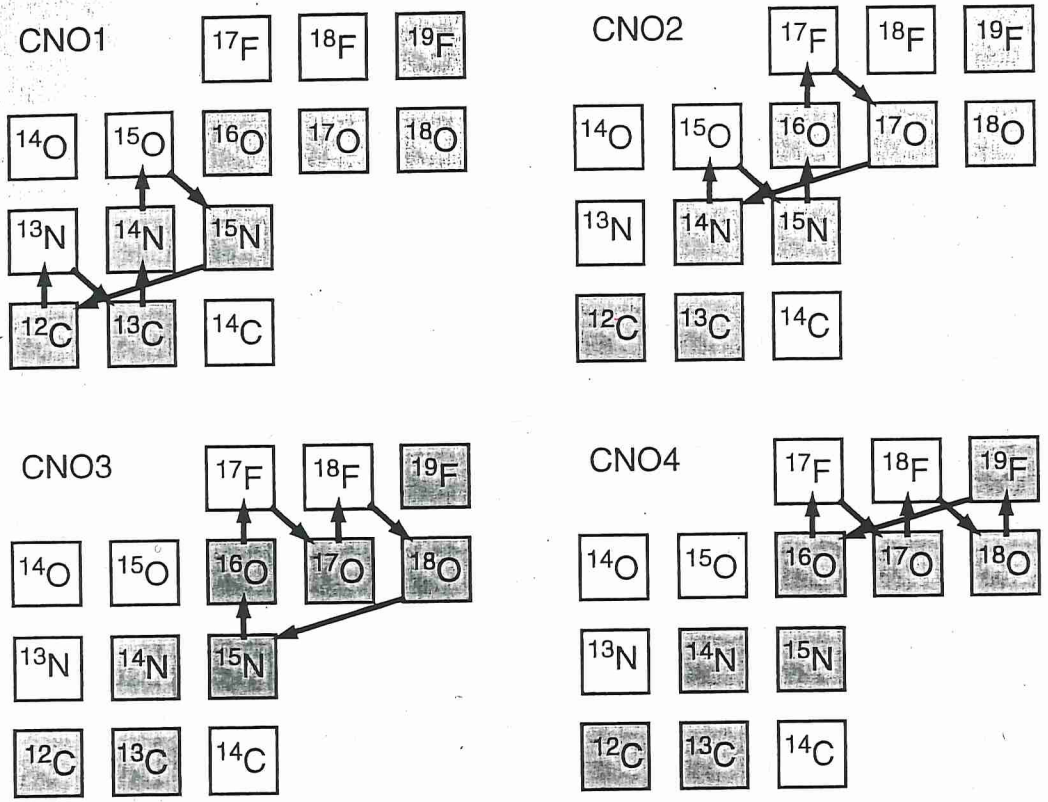

Figure 5.8 Representation of the four CNO cycles in the chart of the nuclides. Stable nuclides are shown as shaded squares. Each reaction cycle fuses effectively four protons to one ^{4}He nucleus.

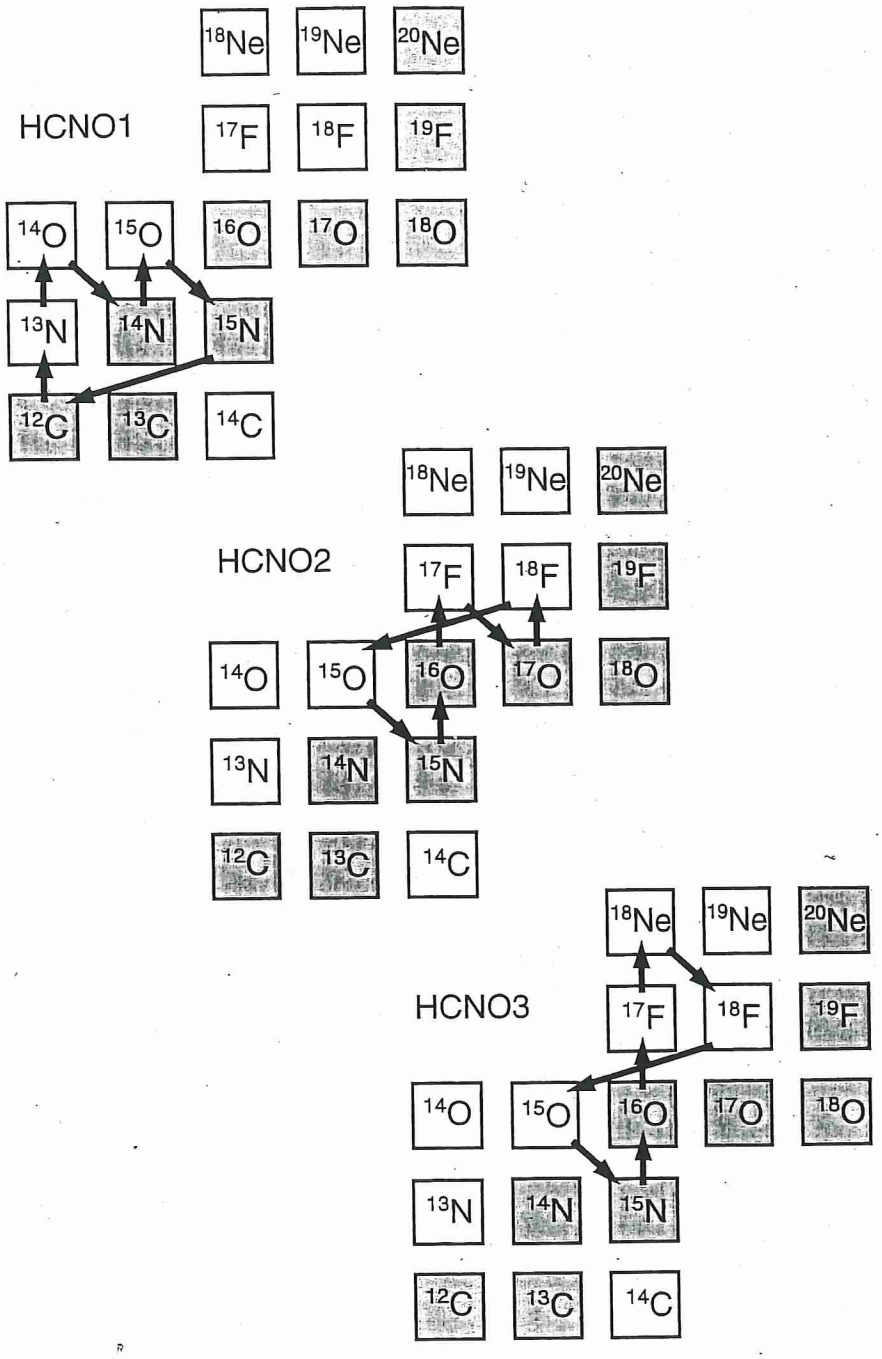

Figure 5.47 Representation of the three hot CNO cycles in the chart of the nuclides. Stable nuclides are shown as shaded squares. Each reaction cycle fuses effectively four protons to one ^{4}He nucleus. In explosive hydrogen burning, the CNO2 cycle (Figure 5.8) is more likely to occur than the HCNO2 cycle since the ^{17}O(p,α)^{14}N reaction rate dominates over the ^{17}O(p,γ)^{18}F rate (Figure 5.9).

LETTER

doi:10.1038/nature14161

Explosive lithium production in the classical nova V339 Del (Nova Delphini 2013)

Akito Tajitsu[1], Kozo Sadakane[2], Hiroyuki Naito[3,4], Akira Arai[5,6] & Wako Aoki[7]

The origin of lithium (Li) and its production process have long been uncertain. Li could be produced by Big Bang nucleosynthesis, interactions of energetic cosmic rays with interstellar matter, evolved low-mass stars, novae, and supernova explosions. Chemical evolution models and observed stellar Li abundances suggest that at least half the Li may have been produced in red giants, asymptotic giant branch (AGB) stars, and novae[1–3]. No direct evidence, however, for the supply of Li from evolved stellar objects to the Galactic medium has hitherto been found. Here we report the detection of highly blue-shifted resonance lines of the singly ionized radioactive isotope of beryllium, ^{7}Be, in the near-ultraviolet spectra of the classical nova V339 Del (Nova Delphini 2013) 38 to 48 days after the explosion. ^{7}Be decays to form ^{7}Li within a short time (half-life of 53.22 days[4]). The ^{7}Be was created during the nova explosion via the alpha-capture reaction ^{3}He(α,γ)^{7}Be (ref. 5). This result supports the theoretical prediction that a significant amount of ^{7}Li is produced in classical nova explosions.

V339 Del (Nova Delphini 2013) is a classical nova that was discovered as a bright 6.8-magnitude (unfiltered) source on 2013 August 14.584 Universal Time (UT)[6]. 40 h after the discovery, a maximum was reached on August 16.25 (Modified Julian Day (MJD) = 56,520.25) at 4.3 magnitude in the Johnson V-band[7]. Then, it began a normal decline.

High-resolution spectra (resolving power $R = 90{,}000$–$60{,}000$) of V339 Del were obtained at four epochs after its outburst (+38 d, +47 d, +48 d, and +52 d). These spectra contain a series of broad emission lines originating from neutral hydrogen (H I, Balmer series) and other permitted transitions of neutral or singly ionized species (for example, Fe II, He I and Ca II). These emission lines are usually seen in post-outburst spectra of classical novae. Most of these broad emission lines are accompanied by sharp and blue-shifted multiple absorption lines at their blue edges. The typical radial velocity (v_{rad}) of these highly blue-shifted absorption lines is about $-1{,}000\ km\ s^{-1}$. Figure 1a and b display the spectrum obtained at +47 d in the vicinities of the H η and Ca II K lines, respectively. The H I line is accompanied by a broad emission with a full-width at half-maximum (FWHM) of $\sim 1{,}300\ km\ s^{-1}$ centred at a radial velocity of $v_{rad} \approx 0\ km\ s^{-1}$. The Ca II K (and H) has a weak but broad emission and strong absorption components caused by the interstellar absorptions. In addition to these profiles around the rest positions of both lines, two sharp absorption components are found at $v_{rad} = -1{,}268 \pm 2\ km\ s^{-1}$ and $-1{,}103 \pm 1\ km\ s^{-1}$. The latter seems to be stronger than the former. Such absorption line systems have been found in post-outburst spectra of several classical novae[8,9]. The absorption line systems in V339 Del contain numerous transitions originating from singly ionized iron-group species (Fe II, Ti II, Cr II, Mn II and Ni II). The depths of all blue-shifted absorption lines in V339 Del are only about 25% or less of the continuum level, while the bottoms of some strong lines (for example, the Balmer lines; see Extended Data Fig. 2) have flat features, suggesting that the absorption is saturated. These observational results can be interpreted as the effect of absorbing materials partially covering the background light source. There are no Na I D doublet lines (at 588.995 nm and 589.592 nm), which are often found to be the strongest absorption features in novae within a few weeks after their outbursts[8,10]. We interpret this as indicating that the ejected gas has evolved into a higher ionization stage before our observing epochs (5–7 weeks after the explosion). The observed spectral energy distribution of this nova indicates that the shape of the continuous radiation had entered a very hot stage (effective temperature >100,000 K) within 5 weeks after the explosion[11]. Other observed characteristics of this nova (for example, light curves, optical and ultraviolet emission lines) show that it is a typical Fe II nova with a carbon–oxygen (CO) white dwarf[12,13].

In these absorption line systems, we noticed two remarkable pairs of absorption features near 312 nm. These correspond to the absorption components originating from transitions at ~313 nm. These pairs are marked A, B and C, D, respectively, in Fig. 1c. Adopting the wavelengths of the resonance doublet lines[14,15] of singly ionized ^{7}Be at 313.0583 nm and 313.1228 nm, we find that features A and B coincide with the $-1{,}103\ km\ s^{-1}$ components of the 313.0583 nm and 313.1228 nm lines, respectively. Similarly, features C and D coincide with the $-1{,}268\ km\ s^{-1}$ components of these two lines. Separations in wavelength between features A and B and between features C and D are consistent with the separation between the doublet lines within the measurement uncertainties. Figure 1d illustrates these coincidences on the velocity scale. The high resolution of the spectrum (~0.0052 nm) means that we can clearly distinguish them from the doublet of ^{9}Be II at 313.0422 nm and 313.1067 nm (ref. 14). After ruling out the possibility of alternative identifications, we conclude that these absorption features at 312 nm are caused by ^{7}Be, and not by ^{9}Be (the only stable isotope of Be). Original ^{9}Be contained in the progenitor star would have been depleted during its evolution because this isotope is destroyed at temperatures $T > 3 \times 10^{6}$ K. On the other hand, production of the unstable isotope ^{7}Be by the reaction ^{3}He(α, γ)^{7}Be in nova explosions has been theoretically predicted[16–21].

The transition probability of the ^{7}Be II line at 313.0583 nm ($\log(gf) = -0.178$, where g is the statistical weight of the lower level and f is the oscillator strength of the transition) is twice as large as that of the ^{7}Be II line at 313.1228 nm ($\log(gf) = -0.479$)[14]. Owing to saturation effects, the ratio of their equivalent widths is expected to be in the range between 2 (no saturation) and 1 (complete saturation). The measured ratios are 1.1 ± 0.3 and 1.6 ± 0.4 for the components at $v_{rad} = -1{,}268\ km\ s^{-1}$ and $-1{,}103\ km\ s^{-1}$, respectively. These are within the range expected for the doublet, although the values contain some errors (within ±25%), mainly because of the uncertainty in the continuum placement. The weaker component at $v_{rad} = -1{,}268\ km\ s^{-1}$ has a ratio closer to complete saturation. This can be interpreted as resulting from the fact that the absorbing gas cloud moving with $v_{rad} = -1{,}268\ km\ s^{-1}$ has a smaller covering factor, and at the same time, a higher column density of ^{7}Be ions than the gas cloud moving with $v_{rad} = -1{,}103\ km\ s^{-1}$.

Figure 2 displays the velocity plots of normalized spectra for different species of the absorption line systems at four observing epochs from +38 d to +52 d after the explosion. On day +38, the ^{7}Be II doublet has

[1]Subaru Telescope, National Astronomical Observatory of Japan, 650 North A'ohoku Place, Hilo, Hawaii 96720, USA. [2]Astronomical Institute, Osaka Kyoiku University, Asahigaoka, Kashiwara, Osaka 582-8582, Japan. [3]Graduate School of Science, Nagoya University, Furo-cho, Chikusa-ku, Nagoya 464-8602, Japan. [4]Nayoro Observatory, 157-1 Nisshin, Nayoro, Hokkaido 096-0066, Japan. [5]Center for Astronomy, University of Hyogo, Sayo-cho, Hyogo 679-5313, Japan. [6]Koyama Astronomical Observatory, Kyoto Sangyo University, Motoyama, Kamigamo, Kita-ku, Kyoto 603-8555, Japan. [7]National Astronomical Observatory of Japan, 2-21-1 Osawa, Mitaka, Tokyo 181-8588, Japan.

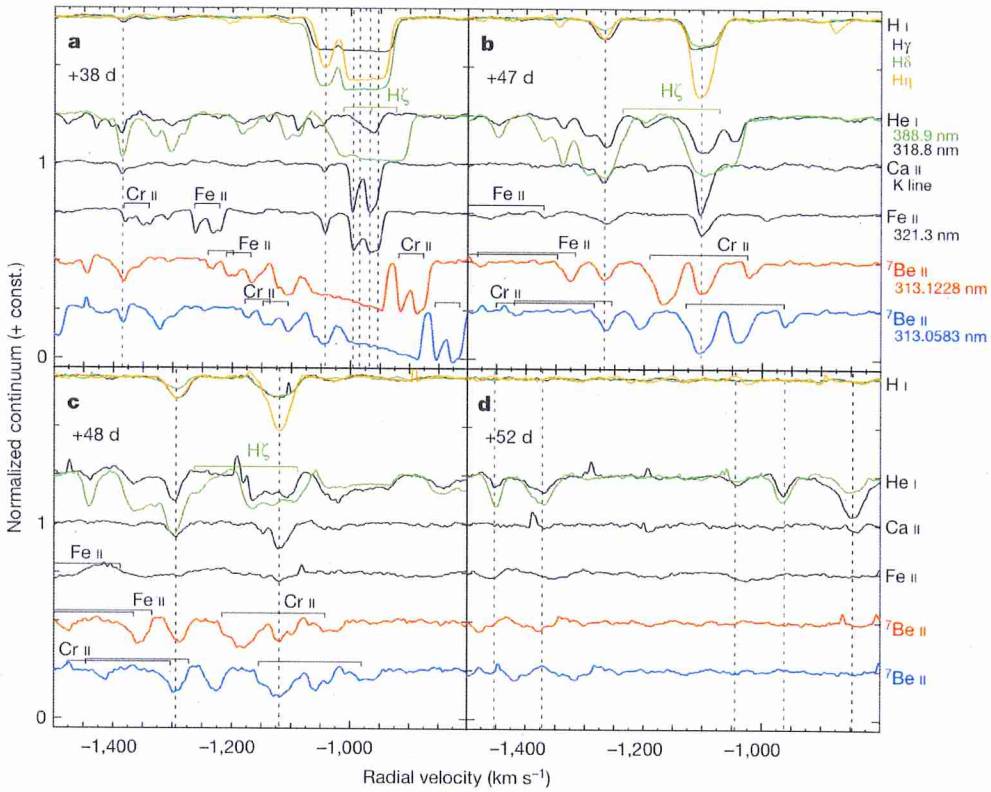

Figure 2 | Time variations of the blue-shifted absorption line systems from day +38 to day +52. Absorption line systems originating from different species at four observing epochs are plotted on the velocity scale. All lines are normalized to the local continuum. Blue-shifted absorption components observed at each epoch are indicated by vertical dashed lines. The identified line or expected line contaminations are labelled above each lines. **a**, On day +38, the profile of the ^{7}Be II doublet around $v_{rad} \approx -1{,}000$ km s^{-1} is complicated, and possibly interpreted as being saturated. **d**, On day +52, no blue-shifted absorption can be found except for the metastable He I lines.

over a long lifetime. Candidates for this, such as low-mass red giants or novae, have been proposed to be major sources of ^{7}Li production (more than half of the Solar System Li, as measured in meteorites) in the Galaxy[1–3]. The production of ^{7}Li in low-mass stars has been theoretically studied[25–29], and Li-enhanced red giants and AGB stars have indeed been identified[30]. The contribution to Li enrichment in the Galaxy by these objects has, however, not been confirmed. This is because the Li-rich phase in these stars might be of quite limited duration and the contribution is dependent upon the mass-loss rate of such objects. Nova eruptions involve a long delay time before working as stellar ^{7}Li factories. This is because ^{3}He-rich low-mass secondaries are necessary to produce ^{7}Be efficiently via the ^{3}He(α, γ)^{7}Be reaction[18]. It is important to know whether this phenomenon is common among classical novae to quantify their contribution to the rapid increase of ^{7}Li in the Galaxy. Since V339 Del appears to be one of the ordinary Fe II type novae that occupy ~60% of all classical novae[12], the ^{7}Be production found in this object might be occurring in many classical novae. Our successful detection of ^{7}Be in V339 Del indicates that measurements of the ^{7}Be lines in the near-ultraviolet range for post-outburst novae within the lifetime of this isotope is a powerful way to estimate the contribution of novae to the chemical evolution of lithium in the Galaxy.

Online Content Methods, along with any additional Extended Data display items and Source Data, are available in the online version of the paper; references unique to these sections appear only in the online paper.

Received 2 September; accepted 16 December 2014.

1. Romano, D., Matteucci, F., Molaro, P. & Bonifacio, P. The galactic lithium evolution revisited. *Astron. Astrophys.* **352,** 117–128 (1999).
2. Romano, D., Matteucci, F., Ventura, P. & D'Antona, F. The stellar origin of ^{7}Li. Do AGB stars contribute a substantial fraction of the local Galactic lithium abundance? *Astron. Astrophys.* **374,** 646–655 (2001).
3. Prantzos, N. Production and evolution of Li, Be, and B isotopes in the Galaxy. *Astron. Astrophys.* **542,** A67 (2012).
4. Audi, G., Bersillon, O., Blachot, J. & Wapstra, A. H. The NUBASE evaluation of nuclear and decay properties. *Nucl. Phys. A* **729,** 3–128 (2003).
5. Cameron, A. G. W. & Fowler, W. A. Lithium and the s-PROCESS in Red-Giant Stars. *Astrophys. J.* **164,** 111–114 (1971).
6. Waagen, E. O. Nova Delphini 2013 = PNV J20233073+2046041. *AAVSO Alert Notice* **489** (2013).
7. Munari, U. *et al.* After a post-maximum plateau Nova Del 2013 has begun a normal decline. *Astron. Telegr.* **5304,** 1 (2013).
8. Williams, R., Mason, E., Della Valle, M. & Ederoclite, A. Transient heavy element absorption systems in novae: episodic mass ejection from the secondary star. *Astrophys. J.* **685,** 451–462 (2008).
9. Sadakane, K., Tajitsu, A., Mizoguchi, S., Arai, A. & Naito, H. Discovery of multiple high-velocity narrow circumstellar NaI D lines in Nova V1280 Sco. *Publ. Astron. Soc. Jpn* **62,** L5–L10 (2010).
10. McLaughlin, D. B. in *Stellar Atmospheres* (ed. Greenstein, J. L.) 585–652 (The University of Chicago Press, 1960).
11. Skopal, A. *et al.* Early evolution of the extraordinary Nova Delphini 2013 (V339 Del). *Astron. Astrophys.* **569,** A112 (2014).
12. Williams, R. E. The formation of novae spectra. *Astron. J.* **104,** 725–733 (1992).
13. Warner, B. Cataclysmic variable stars. *Camb. Astrophys. Ser.* **28,** 257–306 (1995).
14. Kramida, A., Ralchenko, Yu., Reader, J. & the NIST ASD team. *NIST Atomic Spectra Database* Ver. 5.1 http://physics.nist.gov/asd (National Institute of Standards and Technology, 2013).
15. Yan, Z.-C., Nörtershäuser, W. & Drake, G. W. F. High precision atomic theory for Li and Be^{+}: QED shifts and isotope shifts. *Phys. Rev. Lett.* **100,** 243002 (2008).
16. Arnould, M. & Norgaard, H. The explosive thermonuclear formation of ^{7}Li and ^{11}B. *Astron. Astrophys.* **42,** 55–70 (1975).
17. Starrfield, S., Truran, J. W., Sparks, W. M. & Arnould, M. On Li-7 production in nova explosions. *Astrophys. J.* **222,** 600–603 (1978).
18. D'Antona, F. & Matteucci, F. Galactic evolution of lithium. *Astron. Astrophys.* **248,** 62–71 (1991).
19. Boffin, H. M. J., Paulus, G., Arnould, M. & Mowlavi, N. The explosive thermonuclear formation of Li-7 revisited. *Astron. Astrophys.* **279,** 173–178 (1993).
20. Hernanz, M., Jose, J., Coc, A. & Isern, J. On the synthesis of ^{7}Li and ^{7}Be in novae. *Astrophys. J.* **465,** L27–L30 (1996).
21. José, J. & Hernanz, M. Nucleosynthesis in classical novae: CO versus ONe white dwarfs. *Astrophys. J.* **494,** 680–690 (1998).
22. Naito, H., Tajitsu, A., Arai, A. & Sadakane, K. Discovery of metastable helium absorption lines in V1280 Scorpii. *Publ. Astron. Soc. Jpn* **65,** 37 (2013).

METHODS

Discovery. V339 Del (Nova Delphini 2013) is a classical nova that was discovered as a bright 6.8 magnitude (unfiltered) source by Koichi Itagaki on 2013 August 14.584 UT and announced in the American Association of Variable Star Observers (AAVSO) Alert Notice[6]. Its progenitor is estimated to be a blue star (USNO B-1 1107-0509795) with 17.20 magnitude in the Johnson B-band, and 17.45 magnitude in the Cousins R_C-band on the first Palomar Sky Survey Plates (exposed on 1951 July 7), and with $B \approx 17.39$, $R_C \approx 17.74$ on the second Palomar Sky Survey plates (exposed on 1990 July 18 and September 15, respectively)[31]. No significant changes were found in its photometric behaviour for at least a few years before the outburst[32]. On an unfiltered pre-discovery image obtained on 2013 August 13.998 UT, the object was still at 17.1 mag (ref. 33). This means that the object was still in quiescence until at least 14 h before its discovery, and that it showed a very fast rise to the maximum. After 40 h from the discovery, maximum was reached on Aug 16.25 (MJD = 56,520.25) at $V = 4.3$ (ref. 7). Then, it began a normal decline. The nova had been detected as a transient high-energy gamma-ray (>100 MeV) source within about 10 days after the outburst[34]. Angular sizes of the expanding shell around the nova had been monitored until about day +40 using near-infrared interferometric observations[35]. Then, incorporating the expansion velocity obtained in the optical region, the distance to the nova was derived as 4.54 ± 0.59 kiloparsecs from the Sun.

Observations and data reduction. The post-outburst spectra of V339 Del were obtained using the High Dispersion Spectrograph (HDS)[36] of the 8.2 m Subaru Telescope at four epochs from 2013 September 23 to October 7 (+38 d, +47 d, +48 d and +52 d after the maximum). According to the AAVSO light curves (see Extended Data Fig. 1), our first observation was just before the start of the rapid decline in optical magnitudes by dust formation[37]. The following three were obtained during the continuous decline. We obtained spectra under three configurations of the spectrograph, which cover the wavelength regions from 303 nm to 463 nm, from 411 nm to 686 nm, and from 667 nm to 936 nm. The spectral resolving power was set to $R \approx 90{,}000$ or 60,000 with 0.4″ (0.2 mm) or 0.6″ (0.3 mm) slit widths, respectively. The exact times and wavelength ranges of obtained spectra are summarized in Extended Data Table 1. Data reduction was carried out using the Image Reduction and Analysis Facility (IRAF) software in a standard manner. The nonlinearity in the detectors was corrected by the method described in ref. 38. The wavelength calibration was performed using a Th-Ar comparison spectrum and the typical residual in wavelength calibration is about 10^{-4} nm (~0.1 km s^{-1}) or less for each spectrograph configuration. The typical systemic variance of the spectrograph is about 10^{-4} nm or less per hour. We also examined the accuracy of radial velocity determination in our measurement using the identified iron-group transitions in the range 315–351 nm. For the spectrum obtained at day +38, the velocity of the strongest component in the absorption line system was −996.1 ± 0.7 km s^{-1}, determined by Gaussian fittings. In total, we concluded that the residual in our velocity scale determination was ±1 km s^{-1}. Spectrophotometric calibration was performed using the spectrum of BD+28°4211 (ref. 39), obtained at nearly the same nova altitude on the same nights. All spectra were converted to the heliocentric scale. A correction for interstellar extinction has not been applied. The average signal-to-noise ratio in the spectra obtained at four epochs is ~140 at ~312 nm, where we found the ^{7}Be lines.

Highly blue-shifted absorption line system. The spectra of V339 Del exhibit a series of broad Fe II emission lines, which indicate that the object is a typical Fe II type nova[12]. Since no strong emission originating from Ne is found in the spectrum even at day +52, the white dwarf in the system is supposed to be a CO white dwarf[13].

Extended Data Fig. 2a displays the radial velocity profiles of three Fe II belonging to the same multiplet number[40] (42) in the spectrum of day +38. The absorption line system on day +38 clearly consists of five components at $v_{rad} = -954$ km s^{-1}, −968 km s^{-1}, −985 km s^{-1}, −996 km s^{-1}, and −1,043 km s^{-1}, as indicated by the dashed lines in Extended Data Fig. 2b. Similarly, blue-shifted absorption components are found in Balmer lines (Extended Data Fig. 2c) and also in other permitted lines (Ca II H and K, He I at 587.6 nm). In the near-ultraviolet range, numerous absorption lines in the complex continuum are identified as the transitions of singly ionized iron-group species. Most of them belong to the absorption line systems found in the visual region (Extended Data Fig. 3). We applied a Doppler correction using the radial velocity of the strongest blue-shifted absorption line in the system to identify sources of transitions (see Extended Data Fig. 3b). We use the velocities for Doppler corrections as $v_{+38} = -996$ km s^{-1}, $v_{+47} = -1{,}103$ km s^{-1}, and $v_{+48} = -1{,}120$ km s^{-1} for days +38, +47, and +48, respectively (in Extended Data Figs 3b and 4a–c). All of the identified transitions originate from levels of low excitation potential (< 4 eV). The residual intensity at the bottom of these lines exceeds 75% of the continuum, whereas the bottoms of some strong Fe II and Balmer lines show flat structures. These observations suggest that the saturated absorption lines are created by clouds of absorbing gas, which cover only about 25% of the continuum-emitting region.

Very similar short-lived blue-shifted metallic absorption systems have been reported in post-outburst spectra of several classical novae (such as the Transient Heavy Element Absorption; THEA[8]). In particular, the great majority of novae show strong blue-shifted (400–1,000 km s^{-1}) multiple absorption components in the Na I D doublet in the days following their outbursts. In the very slow nova V1280 Sco, multiple high-velocity (700–900 km s^{-1}) absorption components were found in the Na I D doublet even 800 days after its maximum[9]. Although no absorption component of the Na I D is found at any epoch of our observations of V339 Del, other characteristics of the absorption line systems found in V339 Del are quite similar to those of the THEAs in other novae. They are (1) highly blue-shifted (~1,000 km s^{-1}), (2) divided into several velocity components, (3) time variable in their shapes and velocities, and (4) short-lived (2–8 weeks).

Contamination of the ^{7}Be II doublet. We carefully inspected possible contaminations of absorption lines originating from other species to the ^{7}Be II lines, consulting the atomic line database[41]. Extended Data Fig. 4 displays the spectra in the vicinity of the ^{7}Be II doublet obtained at four epochs of our observations. On the spectrum obtained at day +47, there are no candidates that could contaminate the −1,103 km s^{-1} or the −1,268 km s^{-1} components of ^{7}Be II at 313.1228 nm, which we use in our ^{7}Be abundance estimation (see in Extended Data Fig. 4-b).

At this epoch, the other line of the ^{7}Be doublet at 313.0583 nm may be contaminated by some lines originating from iron-group species. We estimate that the −1,268 km s^{-1} component of Cr II (5) at 313.205 nm ($\log(gf) = +0.079$) may contaminate the −1,103 km s^{-1} component of this ^{7}Be II line. The influence of this contamination can be evaluated by applying the line strength ratio between the pair of velocity components of Cr II (5) at 312.497 nm ($\log(gf) = +0.018$) to that of Cr II (5) at 313.205 nm. It is quite small compared with the strength of the ^{7}Be II line (< 5%). Concerning the −1,268 km s^{-1} component of this ^{7}Be II line, we conclude that the weak lines of Fe II (96) at 312.901 nm ($\log(gf) = -2.70$) and Cr II (5) at 312.869 nm ($\log(gf) = -0.32$) do not contaminate severely. This is because similar weak lines of Fe II (82) at 313.536 nm ($\log(gf) = -1.13$) and Cr II (5) at 313.668 nm ($\log(gf) = -0.25$) had completely disappeared until day +47. We can neglect the contamination from the V II (1) line at 313.0257 nm ($\log(gf) = -0.29$), because the other V II (1) line at 312.621 nm ($\log(gf) = -0.27$) is not detected on our spectra.

^{7}Be abundance estimation. We empirically estimate the abundance of ^{7}Be in the absorbing gas by comparing the equivalent widths of the ^{7}Be II line with those of the Ca II K line that are the similar transitions on the atomic energy level diagrams. We assume that the covering factor of the absorbing gas cloud to the background illuminating source has no wavelength dependence. This method could be a simple and robust way to estimate the abundance ratio independently of ejecta models for nova explosions. The estimate, however, includes some uncertainties. One is the difference in the ionization potentials between Be (the first and second ionization potentials; $I_1 = 9.32$ eV, $I_2 = 18.21$ eV) and Ca ($I_1 = 6.11$ eV, $I_2 = 11.87$ eV)[14] that could result in a difference of ionization states between Be and Ca. However, all of the iron-peak elements (Ti to Fe) found in the absorption line systems that have ionization potentials ($I_1 = 6.75$–7.90 eV, $I_2 = 13.58$–18.12 eV) intermediate between those of Be and Ca, are observed only in singly ionized states, suggesting that dominant fractions of Be and Ca are in the singly ionized states, too. In the spectra obtained, we could not find any resonance lines of Sr II or Ba II, which correspond to those of Be II and Ca II. The Sr/Ca and the Ba/Ca number ratios would be quite small, as seen in the solar abundance (much less than 0.001). Another uncertainty is the X(Ca) in the absorption line system. Our assumption that the absorbing gas has the solar X(Ca) should not be far from reality, because the theoretical analysis predicts no overabundance of elements with the mass number >30 in ejecta of CO novae[21]. We remark that our ^{7}Be abundance estimation is carried out using the data obtained at day +47, which is close to the half-life of ^{7}Be (53.22 days). Therefore, the abundance of the freshly produced ^{7}Li in this nova explosion could be twice as high as the $X(^7\text{Be})$ on day +47.

31. Munari, U. & Henden, A. Photometry of the progenitor of Nova Del 2013 (V339 Del) and calibration of a deep BVRI photometric comparison sequence. *Inform. Bull. Variable Stars* **6087,** 1 (2013).
32. Deacon, N. R. *et al.* Pre-outburst observations of Nova Del 2013 from Pan-STARRS 1. *Astron. Astrophys.* **563,** A129 (2014).
33. Denisenko, D. *et al.* V339 Delphini = Nova Delphini 2013 = Pnv J20233073+2046041. *IAU Circ. No.* **9258,** 2 (2013).
34. The Fermi-LAT Collaboration. Fermi establishes classical novae as a distinct class of gamma-ray sources. *Science* **345,** 554–558 (2014).
35. Schaefer, G. H. *et al.* The expanding fireball of Nova Delphini 2013. *Nature* **515,** 234–236 (2014).
36. Noguchi, K. *et al.* High Dispersion Spectrograph (HDS) for the Subaru Telescope. *Publ. Astron. Soc. Jpn* **54,** 855–864 (2002).
37. Shenavrin, V. I., Taranova, O. G. & Tatarnikov, A. M. Dust formation in Nova Del 2013. *Astron. Telegr.* **5431,** 1 (2013).
38. Tajitsu, A., Aoki, W., Kawanomoto, S. & Narita, N. Nonlinearity in the detector used in the Subaru Telescope High Dispersion Spectrograph. *Publ. Natl. Astron. Obs. Jpn* **13,** 1–8 (2010).
39. Massey, P., Strobel, K., Barnes, J. V. & Anderson, E. Spectrophotometric standards. *Astrophys. J.* **328,** 315–333 (1988).

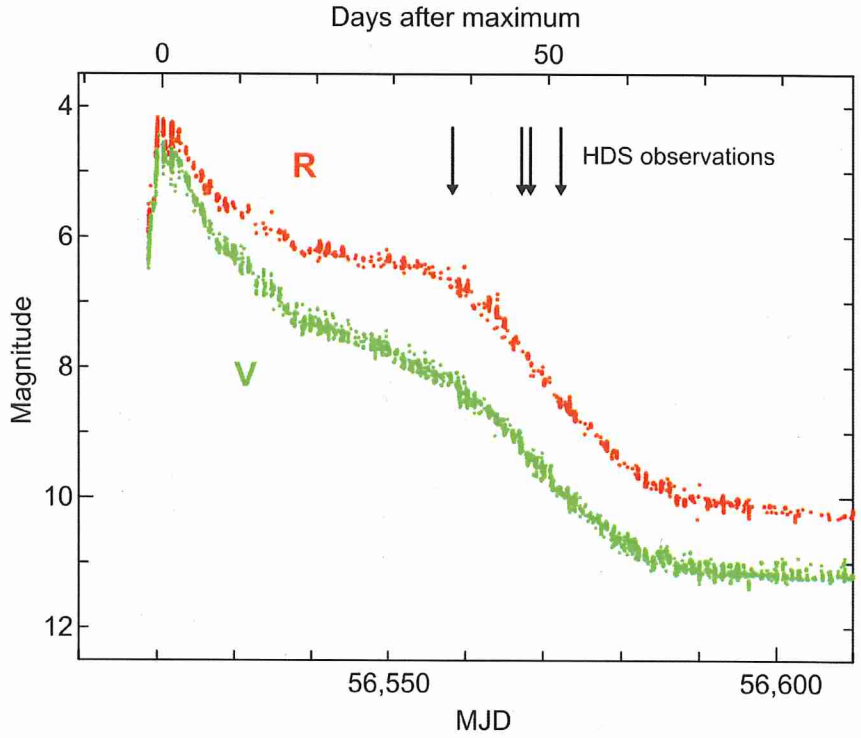

Extended Data Figure 1 | Optical light curves of V339 Del. V (green) and R (red) magnitudes are taken from the AAVSO database. The epochs of our HDS observations are indicated by arrows.

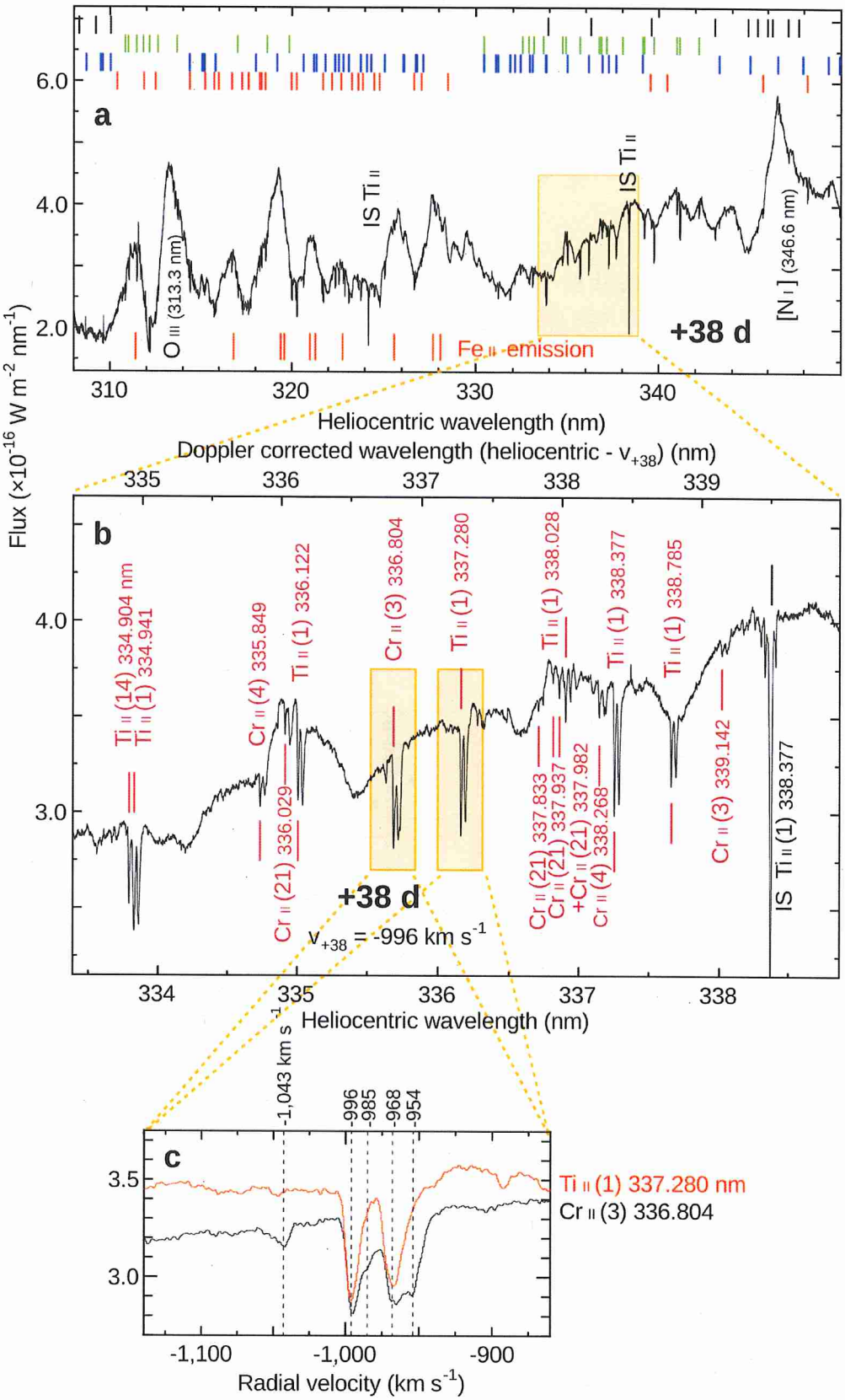

Extended Data Figure 3 | Near-ultraviolet spectrum of V339 Del obtained at day +38. **a**, The overall view of the spectrum from 308 nm to 350 nm. Identified Fe II emission lines are indicated with red ticks at the bottom. The identified absorption line systems originating from iron-group ions are indicated by coloured ticks at the top: Fe II (red), Ti II (blue), Cr II (green), Mn II, Ni II, and V II (black). **b**, A sample of the absorption line identification. The results of our identification are displayed along the spectrum. **c**, As for Extended Data Fig. 2b, but for two lines (Ti II and Cr II), highlighted in **b**, which are plotted on the velocity scale.

Extended Data Table 1 | Journal of HDS observations of V339 Del

Date 2013	UT* (h m)	MJD		Exposure (s)	Range (nm)	Resolution
Sep 23	6 16	56,558.261	(+38 d)†	720	411-686	90,000
	8 12	56,558.342		900	667-936	90,000
	10 07	56,558.423		3,000	303-463	90,000
Oct 02	5 02	56,567.210	(+47 d)†	3,000	303-463	60,000
	6 29	56,567.271		600	411-686	90,000
	7 18	56,567.305		900	667-936	90,000
Oct 03	9 21	56,568.390	(+48 d)†	3,000	303-463	60,000
Oct 07	5 05	56,572.212	(+52 d)†	4,800	303-463	60,000
	7 47	56,572.324		960	411-686	90,000
	8 17	56,572.346		1,500	667-936	90,000

* UT is the universal time at the start of an exposure.
†Days after the optical (V) maximum (MJD = 56,520.25).

DRAFT VERSION JUNE 29, 2015
Preprint typeset using LaTeX style emulateapj v. 01/23/15

EARLY OPTICAL SPECTRA OF NOVA V1369 CEN SHOW PRESENCE OF LITHIUM

LUCA IZZO
Physics Department, Sapienza University of Rome, I-00185; ICRANET, Piazza della Repubblica 10, 65122, Pescara, Italy

MASSIMO DELLA VALLE
INAF, Osservatorio Astronomico di Capodimonte, salita Moiariello 16, 80131, Napoli; ICRANET, Piazza della Repubblica 10, 65122, Pescara, Italy

ELENA MASON
INAF, Osservatorio Astronomico di Trieste, via G.B. Tiepolo 11, I-34143 Trieste, Italy

FRANCESCA MATTEUCCI
Dipartimento di Fisica, Sezione di Astronomia, Universitá di Trieste, via G.B. Tiepolo 11, I-34143 Trieste, Italy

DONATELLA ROMANO
INAF, Osservatorio Astronomico di Bologna, via Ranzani 1, 40127, Bologna, Italy

LUCA PASQUINI
ESO, Karl-Schwarzschild-Strasse 2, 85748 Garching bei Munchen, Germany

LEONARDO VANZI
Department of Electrical Engineering and Center of Astro Engineering, PUC-Chile, Avenida Vicuna Mackenna 4860, Santiago, Chile

ANDRES JORDAN
Institute of Astrophysics and Center of Astro Engineering, PUC-Chile, Avenida Vicuna Mackenna 4860, Santiago, Chile

JOSÉ MIGUEL FERNANDEZ, PAZ BLUHM, RAFAEL BRAHM, NESTOR ESPINOZA
Institute of Astrophysics, PUC-Chile, Avenida Vicuna Mackenna 4860, Santiago, Chile

AND

ROBERT WILLIAMS
Space Telescope Science Institute, 3700 San Martin Drive, Baltimore, MD 21218, USA
Draft version June 29, 2015

ABSTRACT

We present early high resolution spectroscopic observations of the nova V1369 Cen. We have detected an absorption feature at 6695.6 Å that we have identified as blue–shifted ^{7}Li I □6708 Å. The absorption line, moving at -550 km/s, was observed in five high-resolution spectra of the nova obtained at different epochs. On the basis of the intensity of this absorption line we infer that a single nova outburst can inject in the Galaxy $M_{Li} = 0.3 - 4.8 \square 10^{-10} M_{\square}$. Given the current estimates of Galactic nova rate, this amount is sufficient to explain the puzzling origin of the overabundance of Lithium observed in young star populations.
Keywords: novae, cataclysmic variables — Galaxy: abundances

1. INTRODUCTION

The light elements Deuterium, 3-Helium, 4-Helium, and 7-Lithium are synthesized in non-negligible amounts during the first few minutes of the initial cosmic expansion (Kolb & Turner 1990). For Big-Bang Nucleosynthesis in the standard model of cosmology and particle physics (SBBN), the predicted abundances for these elements depends only on one parameter, the baryon-to-photon density ratio. Recently, Planck data have determined the baryon density to excellent precision, leading to a primordial lithium abundance in the range A(Li) = 2:66 - 2:73[1] (Coc et al. 2014). This value is significantly larger than A(Li) □ 2:1 - 2:3 obtained for old metal-poor ([Fe/H] □ - 1:4) halo stars, whose distribution in the Lithium abundance – metallicity diagram is almost flat, and defines the so–called "Spite plateau" (Spite & Spite 1982; Bonifacio et al. 2007). These stars were long thought to share a common, primordial, Li abundance. The discrepancy may be explained by diffusion and turbulent mixing in the stellar interiors (Korn et al. 2006), which corrodes the primordial Li abundance, and/or by a non-standard BBN scenario (Iocco et al. 2009). Yet, another puzzle exists. The abundance

luca.izzo@icra.it - luca.izzo@gmail.com

[1] $A(Li) = \log_{10}(N_{^7Li}/N_H) + 12$

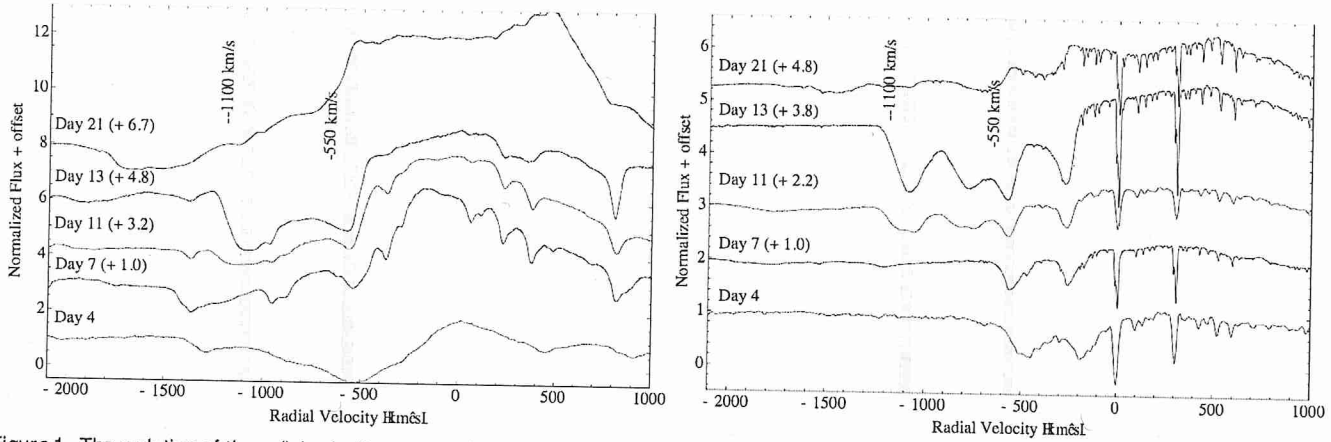

Figure 1. The evolution of the radial velocity systems observed through the P-Cygni profiles in H□ (left panel - centered at □$_{H□}$ = 4861:32) and Na I D2 (right panel - □$_{NaI}$ = 5889:93) lines in the first three weeks of the V1369 Cen outburst. Expansion velocities of -550 and -1100 (□ 30 km/s) are marked with gray rectangles. Note the appearance of multiple expanding systems with increasing time. In particular, the absence in the spectra of day 4 and day 7 of the component at higher velocities (v_{exp} = - 1350 km/s) in the Sodium P-Cygni profile, which is however observed in H□.

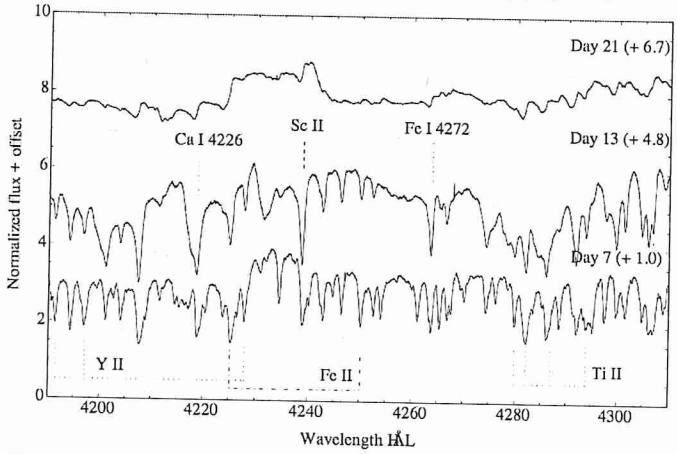

Figure 2. Spectra of V1369 Cen obtained on day 7, 13 and 21 between 4190 and 4310 Å with the identifications of some narrow absorptions lines.

right panel in Fig. 1, no further expanding components are identified for these heavy elements absorbing systems: the cross-correlation method provides a minor number of identifications considering a unique expanding velocity of □ 1100 km/s. If we consider the presence of both expanding components for these heavy elements, the number of acceptable identifications for the higher velocity components is a small fraction □ 1% of the identified lower velocity systems.

Among the many narrow transitions, we have identified many low-ionization neutral elements transitions (Fe, Ca, K), all belonging to the one expanding absorption system at the same velocity that observed in ionized heavy elements, with the only exception being Na I D lines, which show additional expanding components from day 11, see Fig. 1. In particular, we note the clear presence of the resonance transitions of ^{7}Li I 6708, Ca I 4227, and K I 7699, see Fig. 3, all of them with an expansion velocity of v_{exp} □ -550 km/s, in the spectra of day 7 to day 18.

2.1. Possible alternative identifications

Here below we discuss several plausible alternatives to our ^{7}Li identification.

1. We can exclude the possibility that this feature is due to a diffuse interstellar band (DIB – Herbig 1995; Bondar 2012), because i) no known DIBs are located at 6695.6 Å ; ii) all observed heavy elements narrow absorptions vanish after □ 20 days from the initial outburst when the nova continuum is still bright and DIBs should persist, being related to interstellar medium located in between the background exciting radiation and the observer; iii) we observe variations in the observed wavelengths of all these narrow absorptions, an effect that DIBs do not show.

2. An other possibility that must be considered is whether the 6695.6 Å absorption line is due to metal lines excited by resonance absorption of UV radiation which is absorbed in the iron curtain phase and then reprocessed at longer wavelengths (Johansson 1983; Shore 2012). For example, each of the resonance transitions of Li, Ca, and K could be alternatively identified with a transition of Fe or an s-process element at that wavelength, assuming that they are pumped by UV radiation (either continuum or lines). Particularly for the Li I 6707.8 Å resonance doublet, a possible identification could be Fe II 6707.54 Å . In this case one should also expect absorption features from the same lower energy level configuration ($3d^6(^5D)5p$), and from the same term (4Fo - 4G), which results in additional 2 other possible transitions (Fe II 6769.27, 6811.49 Å) in the observed spectra. We have checked for[5] their presence in the spectra of day 7 and day 13[6], but we did not find any absorption feature corresponding to Fe II 6769.27 and 6811.49 Å . This evidence disfavours an UV-pumped origin for the absorption at 6695.6 Å , even if considering the coupling between the transitions and the ejecta velocity field. Conversely, it supports our initial identification as expanding Li I 6708 Å.

3. We compare the red spectral region of Nova Cen with the same region observed in GW Ori, a T Tauri star characterized by the presence of Lithium (Bonsack & Greenstein 1960). GW Ori was observed with FEROS and we have selected the observation of 26 November 2010. In Fig. 4 we show the comparison of these two spectra, after correcting the nova spectrum for the expanding velocity of v_{exp} = - 550 km/s. We clearly see the presence in the GW Ori of broad Ca I 6718 Å and Li I 6708Å giving more support to the identification of absorptions at 6695.6 Å and 6705.3 Å detected in V1369, with Li I 6708 and Ca I 6718.

[5] we consider a □ □ = j□$_{obs}$ - □$_{labj}$ □ 0.4 Å.

[6] these epochs corresponds to the first two FEROS observations, which show the largest number of narrow absorptions, due also to a greater resolution, in our entire spectral database

therefore fast novae, which can form □ 30% of the nova population of the Milky Way (Della Valle & Duerbeck 1993), should contribute only marginally to the global ^{7}Li yield. The above reported range of lithium mass decreases to $M_{Li;tot}$ □ 17 $M_{\odot}$/Gyr, for a rate of "slow" novae of 15-24 events/year, in good agreement with the theoretical predictions (José & Hernanz 1998).

In Fig. 5 it is shown the A(Li) vs. [Fe/H] observed relation compared with Galactic chemical evolution model results. The Galactic chemical evolution model used is an updated version of the chemical evolution model of Romano et al. (1999, 2001), that is based on the two-infall model of Chiappini et al. (1997), and that includes AGB stars (Karakas 2010), super-AGB stars (Doherty et al. 2014a), Galactic cosmic rays (Lemoine et al. 1998) and novae, as Li producers. In this model, the Galactic inner halo and thick disc form by accretion of gas of primordial chemical composition on a short timescale (□ 1 Gyr). The gas is efficiently turned into stars as long as its density is above a critical threshold, below which the star formation stops. The thin disc forms out of a second episode of infall of gas of mainly extragalactic origin on longer timescales (7-8 Gyr in the solar neighborhood) and with lower star formation efficiency. It is worth emphasizing that the adopted mass assembly history is consistent with what is obtained for Milky Way-like galaxies in a full cosmological framework (Colavitti et al. 2008). The black continuous line in Fig. 5 is the best fit to the data obtained with a model with all Li sources, starting from a primordial Li abundance of A(Li) = 2:3 and by assuming that each "slow" nova (the adopted current slow novae rate is 17 events/yr) ejects on an average M_{Li} = 2.55 □ 10^{-10} $M_{\odot}$ in agreement with the measurement of M_{Li} = 0.3 - 4.8 □ 10^{-10} $M_{\odot}$ presented in this paper. The black dashed line shows the predictions of the same model when a high primordial Li abundance is adopted (see the Introduction). The red line is the best model with all Li factories but novae: it is clearly seen that novae are necessary to explain the late rise from the plateau value. The grey area indicates the uncertainties in the model predictions due to uncertainties in both the estimated Li yield from novae and the current slow nova rate: the upper (lower) boundary refers to the upper (lower) limit to the Li yield estimated in this paper and a maximum (minimum) current slow nova rate of 24 (15) events/yr. The light green area similarly indicates the uncertainties in the model predictions when the maximum and minimum Li yields from José & Hernanz (1998) are assumed. Though the two areas partly overlap, it is clearly seen that the theoretical nova yields tend to underproduce Li in the Galaxy, while the semi-empirical yields estimated in this paper give a better match with observed data points. Should the result presented here be confirmed by further observations of ^{7}Li, Classical novae would stand as one of the major Li producers on a Galactic scale.

We thank the referee for her/his constructive comments/criticisms which have improved the paper and Steven Shore, Marina Orio and Paolo Molaro for useful discussions. We are grateful to Roland Gredel for DDT programme 091.A-9032 B. We acknowledge support by project Fondecyt n. 1130849.

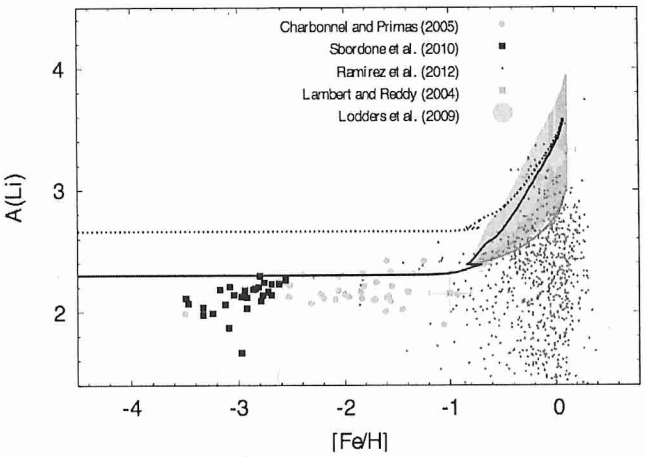

Figure 5. A(Li) vs [Fe/H] for solar neighbourhood stars and meteorites (symbols – see legend) compared to the predictions of chemical evolution models (lines and coloured areas). The back and forth behavior in the theoretical curves around [Fe/H]=- 0.8 is due to the transition between the halo/thick-disc and thin-disc formation phases (see text).

REFERENCES

Bode, M. F., & Evans, A. 2008, Classical Novae.
Bondar, A. 2012, MNRAS, 423, 725
Bonifacio, P., Molaro, P., Sivarani, T., et al. 2007, A&A, 462, 851
Bonsack, W. K., & Greenstein, J. L. 1960, ApJ, 131, 83
Brandi, E., Quiroga, C., Mikołajewska, J., Ferrer, O. E., & García, L. G. 2009, A&A, 497, 815
Cameron, A. G. W., & Fowler, W. A. 1971, ApJ, 164, 111
Charbonnel, C., & Primas, F. 2005, A&A, 442, 961
Chiappini, C., Matteucci, F., & Gratton, R. 1997, ApJ, 477, 765
Coc, A., Uzan, J.-P., & Vangioni, E. 2014, JCAP, 10, 50
Colavitti, E., Matteucci, F., & Murante, G. 2008, A&A, 483, 401
D'Antona, F., & Matteucci, F. 1991, A&A, 248, 62
Della Valle, M., & Duerbeck, H.W. 1993, A&A, 271, 175
Della Valle, M., & Livio, M. 1994, A&A, 286, 786
Della Valle, M., & Livio, M. 1995, ApJ, 452, 704
Della Valle, M., Pasquini, L., Daou, D., & Williams, R. E. 2002, A&A, 390, 155
Doherty, C. L., Gil-Pons, P., Lau, H. H. B., et al. 2014a, MNRAS, 441, 195
Friedjung, M. 1979, A&A, 77, 357
Herbig, G. H. 1995, ARA&A, 33, 19
Iben, Jr., I. 1973, ApJ, 185, 209
Iocco, F., Mangano, G., Miele, G., Pisanti, O., & Serpico, P. D. 2009, Phys. Rep., 472, 1
Johansson, S. 1983, MNRAS, 205, 71P
José, J., & Hernanz, M. 1998, ApJ, 494, 680
Karakas, A. I. 2010, MNRAS, 403, 1413
Kaufer, A., Stahl, O., Tubbesing, S., et al. 1999, The Messenger, 95, 8
Kolb, E. W., & Turner, M. S. 1990, The early universe.
Korn, A. J., Grundahl, F., Richard, O., et al. 2006, Nature, 442, 657
Kramida, A., Ralchenko, Y., Reader, L., & the NIST ASD team, 2013, NIST Atomic Spectra Database Ver. 5.1 http://physics.nist.gov/asd
Lambert, D. L., & Reddy, B. E., 2004, MNRAS, 349, 757L
Lemoine, M., Vangioni-Flam, E., & Cassé, M. 1998, ApJ, 499, 735
Livio, M., & Truran, J. W., 1987, ApJ, 318, 316
Lodders, K., Palme, H., & Gail, H.-P. 2009, Landolt Börnstein, 44
Mason, E., Della Valle, M., Gilmozzi, R., Lo Curto, G., & Williams, R. E. 2005, A&A, 435, 1031
Prantzos, N. 2012, A&A, 542, A67
Prialnik, D., & Kovetz, A. 1995, ApJ, 445, 789
Romano, D., Matteucci, F., Molaro, P., & Bonifacio, P. 1999, A&A, 352, 117
Romano, D., Matteucci, F., Ventura, P., & D'Antona, F. 2001, A&A, 374, 646
Sbordone, L., Bonifacio, P., Caffau, E., et al. 2010, A&A, 522, 26
Shafter, A. W. 1997, ApJ, 487, 226
Shore, S. N. 2012, Bulletin of the Astronomical Society of India, 40, 185
Shore, S. N., Wahlgren, G. M., Augusteijn, T., et al. 2011, A&A, 527, A98
Spite, F., & Spite, M. 1982, A&A, 115, 357
Spitzer, L. J., 1998, Physical Processes in the Interstellar Medium.
Starrfield, S., Truran, J. W., Sparks, W. M., & Arnould, M. 1978, ApJ, 222, 600
Tajitsu, A., Sadakane, K., Naito, H., Arai, A., & Aoki, W. 2015, Nature, 518, 381
Travaglio, C., Randich, S., Galli, D., et al. 2001, ApJ, 559, 909

NEUTRON STARS + X-RAY BURSTS

- X-ray bursts discovered when satellites with good timing up.
- NEUTRON STAR with accretion from a companion
- accretion onto NS
  → 200 MeV/nucleon
  → $T_{NS} \sim 10^7$ K
- BURST → 10^{39} ergs a few seconds
  & REPEATS
- RISE steeper than FALL
- 'BLACK BODY' FLUX → AREA of burst. GROWS AS BURST PROCEEDS (OCEANS OF ^{56}Ni ON NS CRUST)

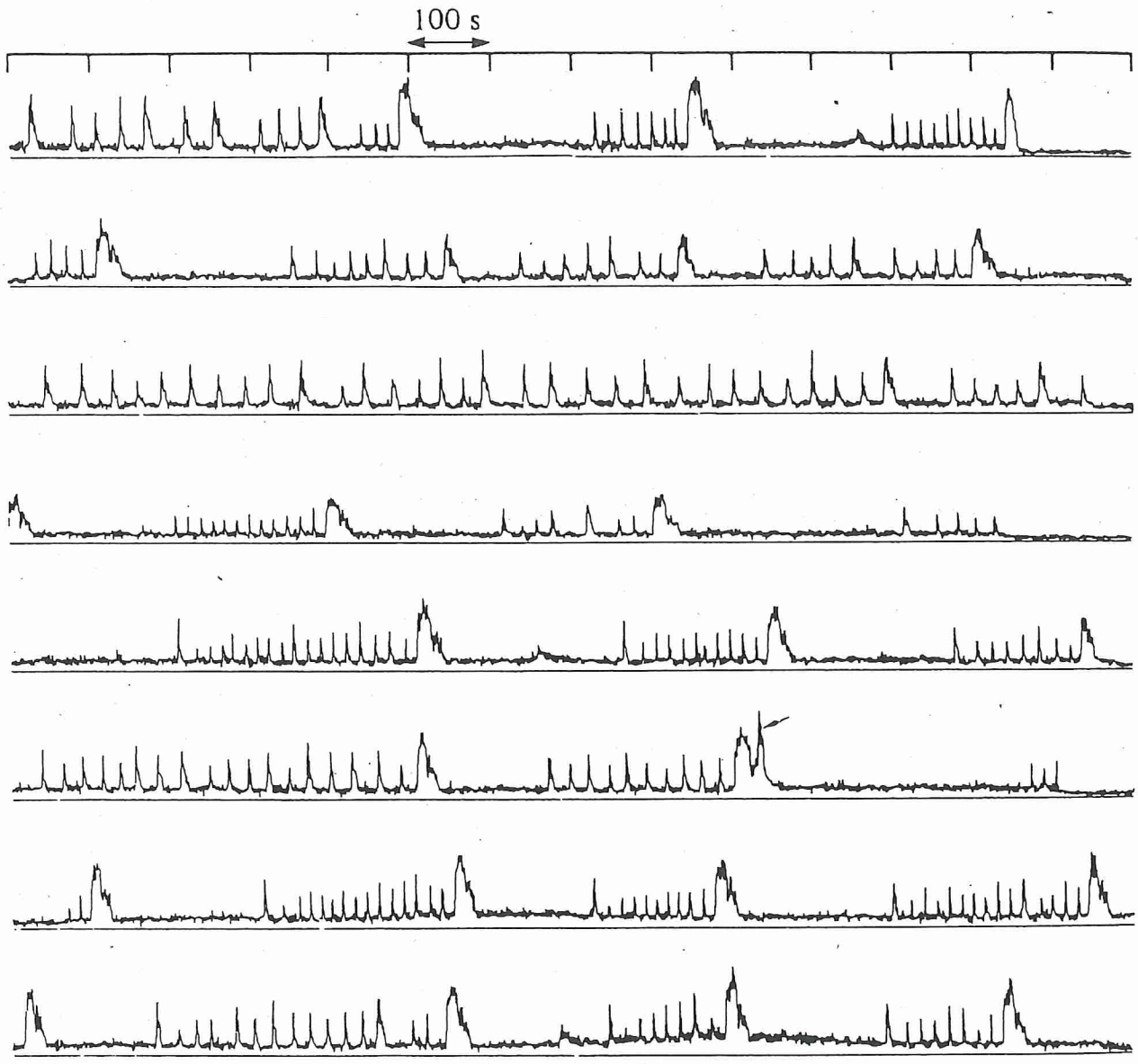

Fig. 5.4 Type II bursts from the Rapid Burster, based on SAS-3 observations performed in march 1976. The burst pinpointed with an *arrow* is actually a type I burst. Image from Lewin (1977)

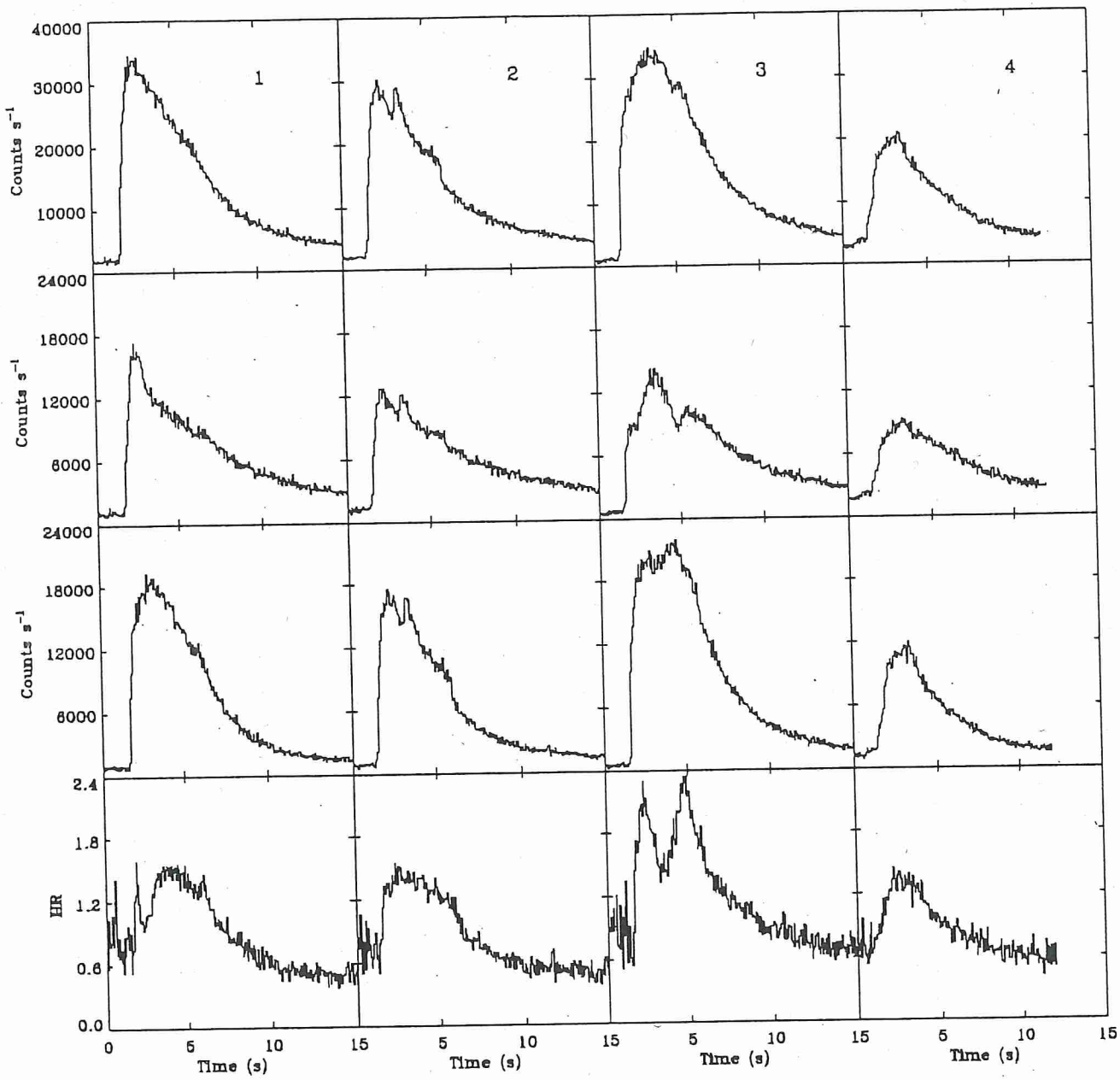

Fig. 5.5 A suite of XRB lightcurves from the LMXB source 4U1728-34 as observed with the RXTE satellite. Each sequence (top to bottom), shows the overall count rates in the energy bands 2–60 keV, 2–6 kev, 6–30 keV, and the ratio (6–30 keV)/(2–6 keV). Figure from Strohmayer and Bildsten (2006)

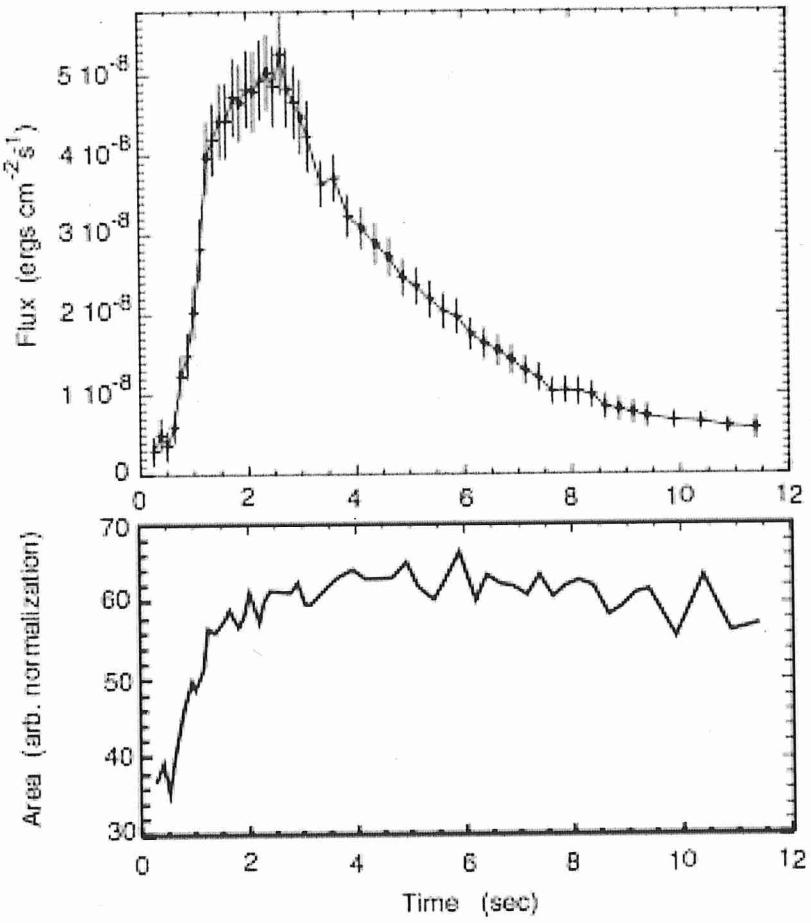

Figure 13. A thermonuclear x-ray burst from the neutron star in the low-mass x-ray binary system 4U 1728–34, as observed with the Rossi x-ray timing explorer. The top shows the rapid increase of the x-ray flux, followed by a slower decay. The lower panel indicates the change of the x-ray emitting area calculated for blackbody radiation from a specical system. The initial increase of the area provides strong evidence of the spread of the nuclear burning front over the entire surface of the neutron star (courtesy: Tod Strohmayer).

ENERGETICS

ACCRETION → 200 MeV/nucl

BURST energy from Nuclear fusion ~ 5 MeV/nucl.

∴ STORAGE and then BURST

SITE

THIN SHELL ON NEUTRON STAR

$T_9 \sim 1$

INSTABILITY → BURST

GRAV. ATTRACTION bal. by RADIATION PRESSURE

T such that H & He burning occur simultaneously

ACCRETION

→ CNO-cycling prior to burst

$\dot{m}$ - slow & burning = stable

$\dot{m}$ ~ not so slow : burning unstable ⇒ X-ray burst

depends on CNO abundance

- He-burning: v. T sensitive
- H-burning (+ CNO): not so T sensitive

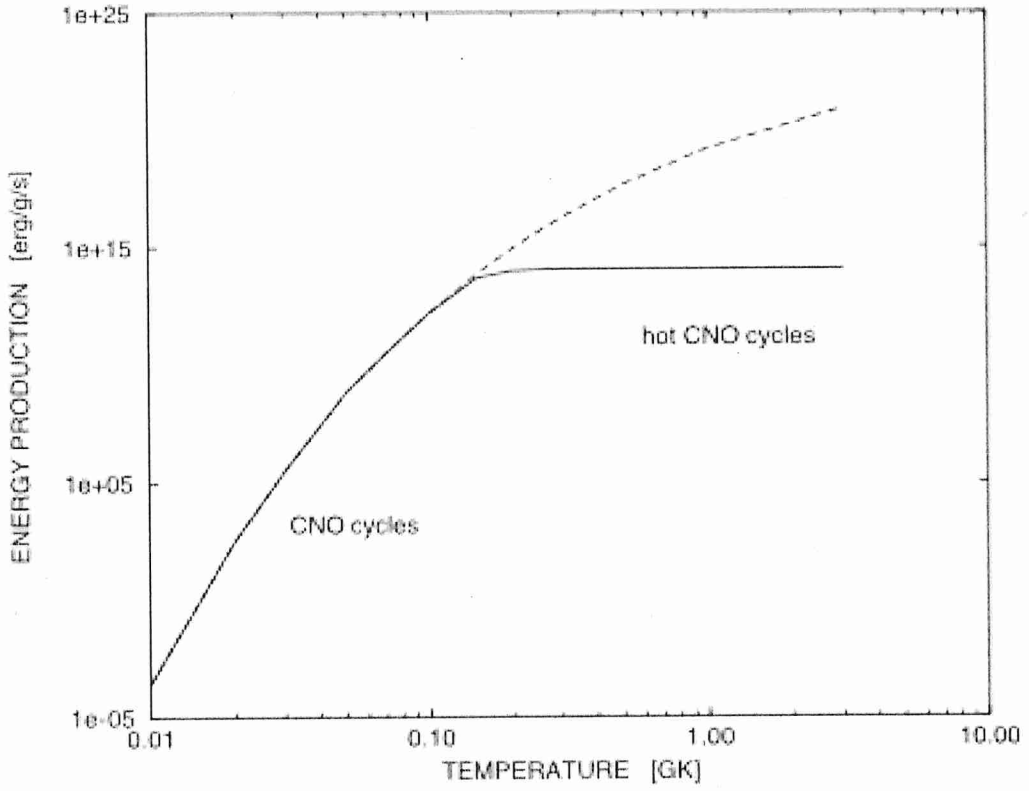

Figure 5. Energy production in the CNO cycles as a function of temperature calculated for a typical stellar density of $\rho = 100$ g cm^{-3}. At lower temperatures (cold CNO cycles) the energy generation is limited by the ^{14}N(p, γ)^{15}O reaction rate and is given by equation (7) (dashed curve), at higher temperatures (hot CNO cycles) the energy generation is limited by the β-decay rates of ^{14}O and ^{15}O.

The nuclear trigger of X-ray Bursts

break-out from HCNO cycles: $^{15}O(\alpha,\gamma)^{19}Ne$

$^{18}Ne(\alpha,p)^{21}Na$

Reaction rate determined by single resonance

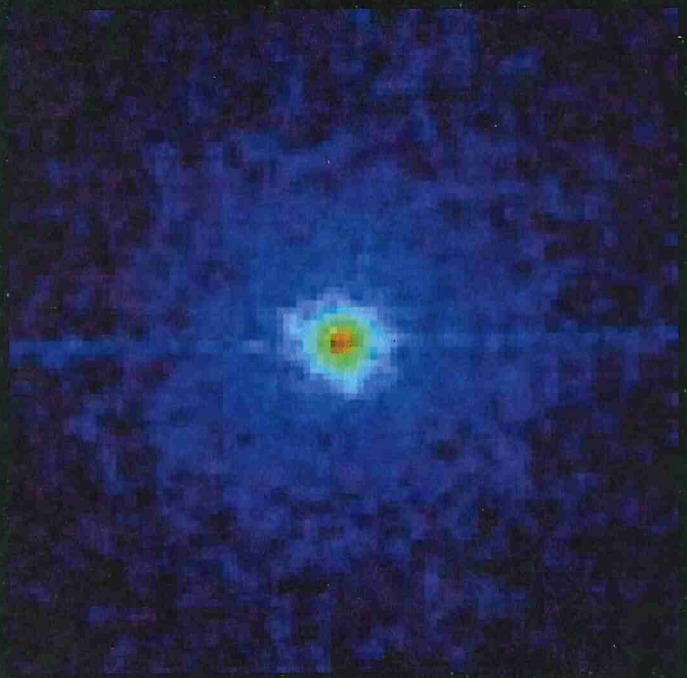

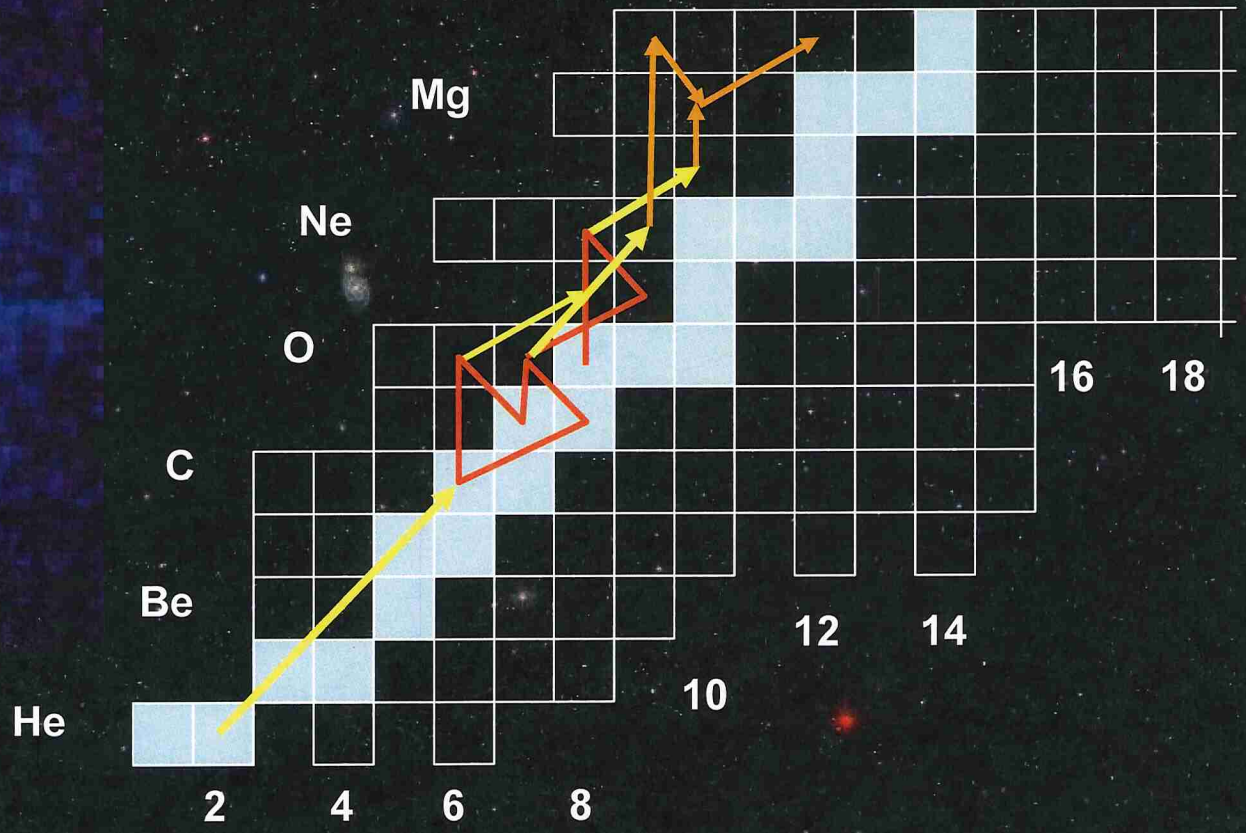

rp-Process

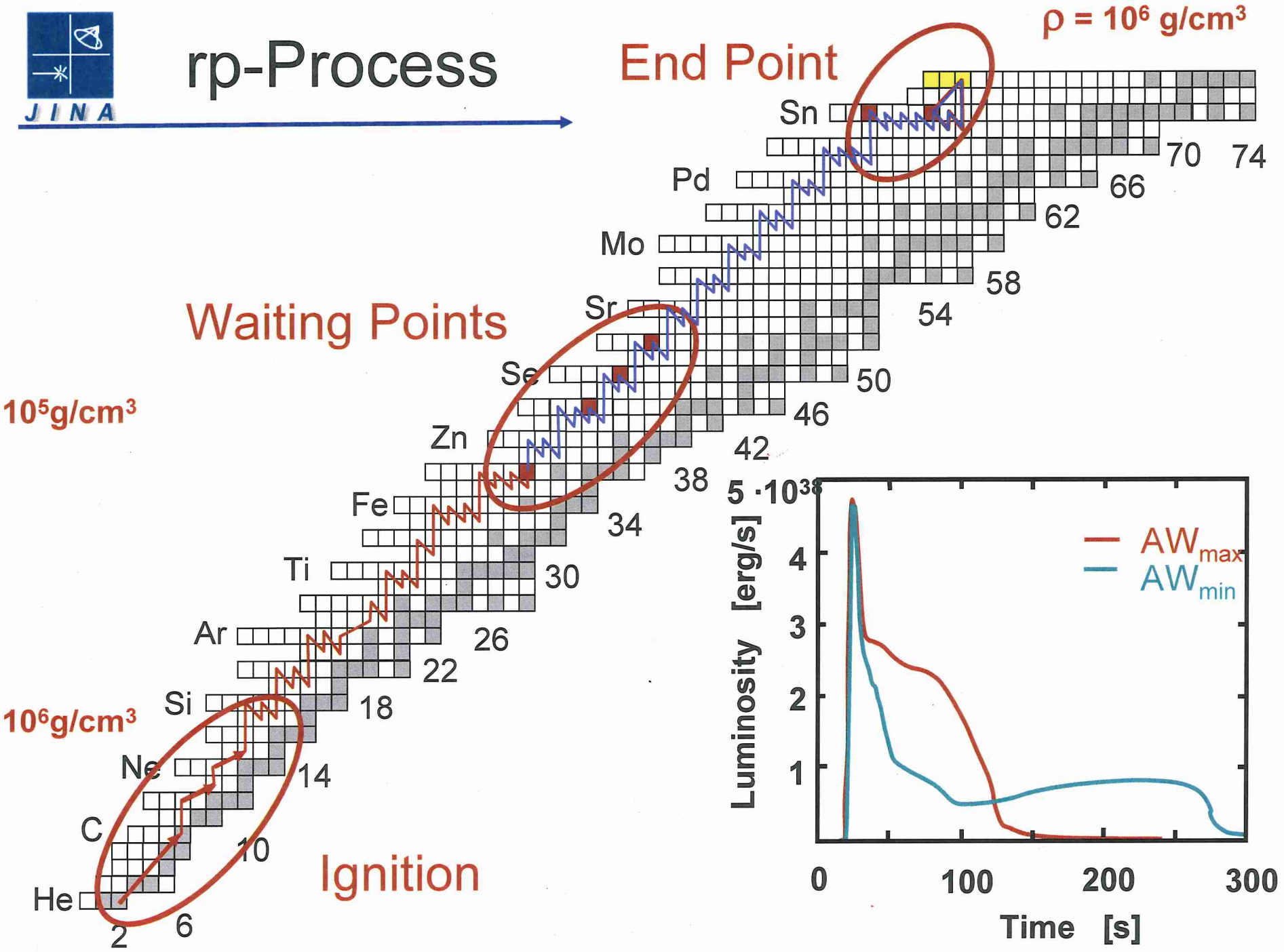
ρ = 10⁶ g/cm³
End Point
Waiting Points
10⁵g/cm³
10⁶g/cm³
Ignition
Sn
Pd
Mo
Sr
Se
Zn
Fe
Ti
Ar
Si
Ne
C
He
74
70
66
62
58
54
50
46
42
38
34
30
26
22
18
14
10
6
2
5 ·10³⁸
4
3
2
1
Luminosity [erg/s]
AW_max
AW_min
0
100
200
300
Time [s]

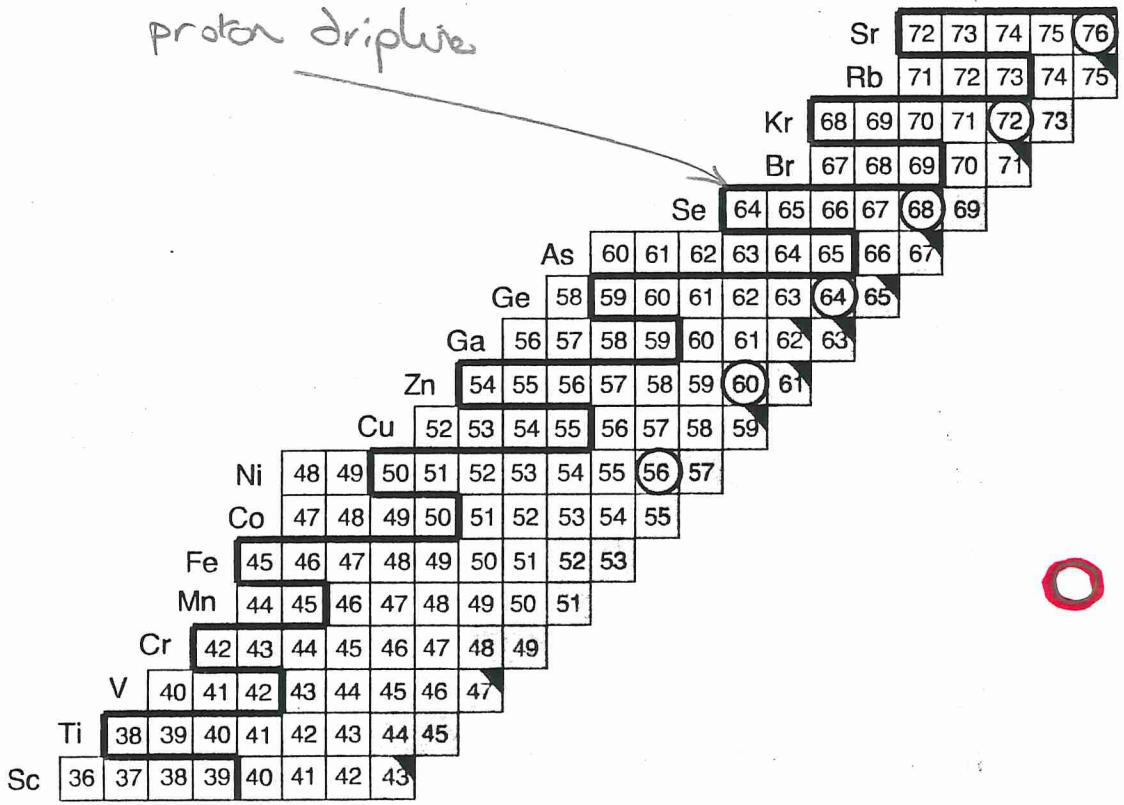

O = waiting points

N=Z?

Fig. 5.35 Section of the chart of the nuclides between Sc ($Z = 21$) and Sr ($Z = 38$) on the proton-rich side of the stability valley. The proton dripline according to Audi, Wapstra and Thibault (2003) is marked by a thick solid line. All displayed nuclides are unstable. Those represented by shaded squares have half-lives in excess of $T_{1/2} \approx 10$ s, while all other nuclides have half-lives of less than $T_{1/2} \approx 3$ s. Nuclides with negative or small positive $Q_{p\gamma}$-values and relatively long β^+-decay half-lives are marked by circles (waiting point nuclei). The solid triangles indicate nuclides for which both the (p,γ) and (p,α) reaction channels are open.

BURST NUCLEOSYNTHESIS

- FUEL (H, He) SUPPLY MAY BE EXHAUSTED BEFORE N's IS FINISHED
- NUCLEAR PHYSICS CONSTRAINTS
  - WAITING POINTS

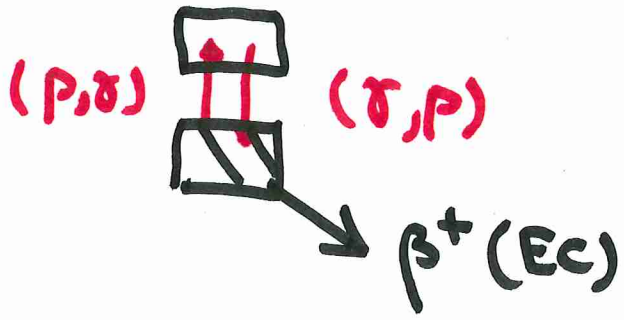

e.g. ^{68}Se
$\tau_\beta = 36^s$

  - BREAKOUT

$^{15}O(\alpha,\gamma)^{19}Ne$
$^{18}Ne(\alpha,p)^{21}Na$ — (αp)-process
$^{18}F(p,\gamma)^{19}Ne$ — (rp)-process

  - ^{56}Ni BOTTLENECK

- CYCLES

  NeNa, MgAl, SiP, SCl,

  ArK, CaSc,

  "IMPEDANCE" (p,α) to (p,γ) rate

- END POINT (unless fuel remains first)

  Sn - Sb - Te cycle

- NUCLOSYNTHESIS (ILIADIS)

  YES — but — ejected?

  radiation driven wind?